IEEE Access
Multidisciplinary ⋮ Rapid Review ⋮ Open Access Journal

Received 23 December 2022, accepted 5 January 2023, date of publication 11 January 2023, date of current version 23 January 2023.

Digital Object Identifier 10.1109/ACCESS.2023.3235924

TOPICAL REVIEW

Three-Port Converters for Energy Conversion of PV-BES Integrated Systems–A Review

MD. MEJBAUL HAQUE[1,2], (Senior Member, IEEE), PETER J. WOLFS[2], (Senior Member, IEEE), SANATH ALAHAKOON[2], (Member, IEEE), MD. ARIFUL ISLAM[3], MITHULAN NADARAJAH[1], (Senior Member, IEEE), FIRUZ ZARE[3,4], (Fellow, IEEE), AND OMAR FARROK[3], (Member, IEEE)

[1]School of Information Technology & Electrical Engineering, The University of Queensland, Brisbane, QLD 4067, Australia
[2]College of Engineering & Aviation, CQUniversity, Rockhampton, QLD 4701, Australia
[3]Department of Electrical and Electronic Engineering, Ahsanullah University of Science and Technology, Dhaka 1208, Bangladesh
[4]School of Electrical Engineering and Robotics, Queensland University of Technology, Brisbane, QLD 4000, Australia

Corresponding author: Md. Mejbaul Haque (mejbaul.haque@uq.edu.au)

ABSTRACT The integration of battery energy storage (BES) with photovoltaic (PV) systems is becoming economically attractive for residential customers. The conventional approach for the interconnection of PV and battery systems requires at least two separate power converters that results in multistage power conversion for some power flows. The dc-dc three port converters (TPCs) are an alternative solution. These converters have many topological variants and possess different operating principles, topological benefits and limitations, and complexities. This paper concentrates on the topological study of TPCs for integrated PV and BES systems applications in the power range from a few hundred watts to 350 kW. These are classified into three different categories based on their isolation features between the ports to establish a topological mapping of the reported TPCs. This provides a framework that systematically explores the full range of technical benefits and limitations of each TPC topology. This paper also examines the possible extension of the TPC topologies for grid-interactive PV-BES systems where bidirectional power flow capability is required between grid and BES systems. This extensive review will provide a useful framework and a strong point of reference for researchers for the selection of TPC topologies to meet the system requirements for PV and energy storage applications.

INDEX TERMS Battery energy storage, energy conversion, modulation and control, photovoltaic, isolated three-port converter, non-isolated three-port converter.

I. INTRODUCTION

PV is one of the major renewable energy sources (RES) [1], [2]. The transition towards a zero emission, dynamic and resilient power system could be effectively accelerated by integrating more RES and BES systems across the network [3]. According to the International Energy Agency (IEA) Photovoltaic Power Systems Programme (PVPS) report, the total global installed capacity of solar PV systems is 1160 GW with an annual installation rate of 220 GW in 2022 [4], [5]. A large part of these PV systems is being installed as small-scale rooftop PV installations at residential premises. Fig. 1 shows the global cumulative PV systems installation capacity over the ten year period from 2012-2022.

In Australia, PV installations are mostly residential in the form of rooftop solar PV, but there are also a growing number of commercial rooftop systems. The total global BES systems capacity in stationary applications is currently estimated to be 11 GWh and could increase to between 100 GWh and 167 GWh in 2030 [7]. These are largely residential BES systems. The operational flexibilities of the increased grid penetration of the RES could be potentially optimized by combining energy storage systems such as residential, commercial or community owned BES systems. As the unit

The associate editor coordinating the review of this manuscript and approving it for publication was Branislav Hredzak.

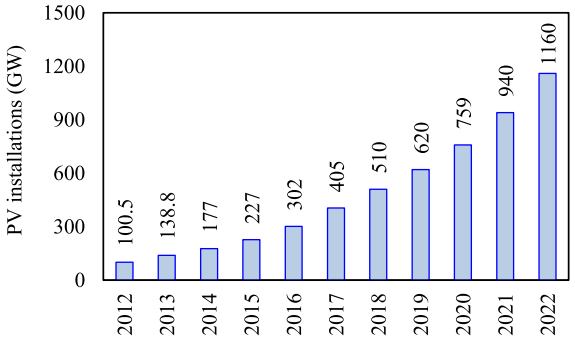

FIGURE 1. Total global cumulative installed PV capacity (2012-2022) [4], [6].

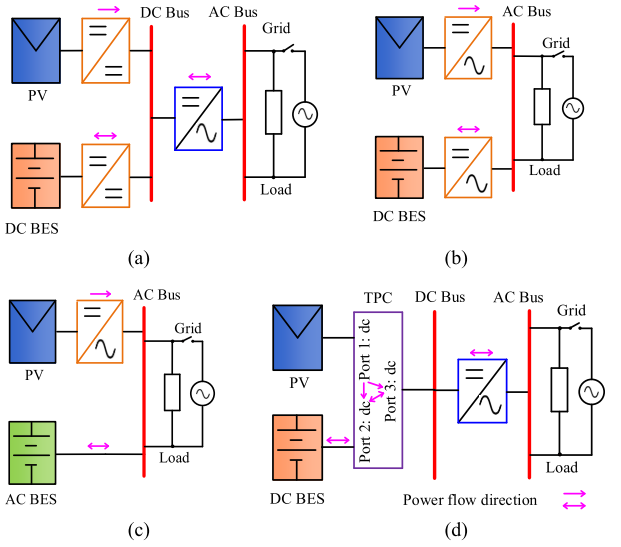

FIGURE 2. Basic topological structures for integrating PV and BES systems (a) two two-port dc-dc converters with a dc bus, (b) two two-port dc-ac converters with an ac bus, (c) a two-port dc-ac converter and an integrated ac battery system with an ac bus, (d) an integrated TPC with a dc bus.

cost of lithium-ion-based BES systems drops gradually, the penetration of integrated PV and BES systems can be significantly expanded across the network [8] to mitigate the erratic behavior of RES such as PV systems. An increasing trend of BES systems deployment in the energy sector is forecasted due to their significant price reduction by 2030 [8]. The BES systems are mostly rated against their output voltage and ampere-hour capacity. The ratings are standardized for commercial and industrial applications that may not match the PV systems ratings. To support the potential expansion of the PV and BES systems, efficient and improved converter topologies are essential. The integration of BES with PV systems can be achieved by multiple converter approaches. However, the growing concern is the cost of power electronics converters. The Little Box challenge is an example of an international contest to develop very compact and low cost conversion technologies [9]. Also, the deployment of multiple converters in energy conversion for PV and BES integrated systems reduces the overall efficiency due to multistage power conversion and increases total system cost [10], [13]. In addition, this requires an overarching control and communication system for power flow management. Communication delay and errors will adversely affect control performance [12], [14]. An alternative may be a multiport converter, which allows arbitrary energy flows between three or more ports and can be used to accommodate multiple energy sources and energy storage devices.

Ideally this should have features such as compactness, reduced cost, flexible centralized power flow control, and high efficiency and power density due to the reduced numbers of conversion stages [15]. The PV and BES (dc/ac) systems can be connected with loads/ac grids in a variety of ways using power converters. The four possible topological configurations for integrating PV and BES systems are shown in Fig. 2. Fig. 2(a) shows a topology for a dc-coupled PV and BES hybrid system. This topology requires two individual two port converters for the PV array and battery, and the systems are connected with the regulated dc bus. This is often termed a dc coupled BES system. This system requires a dc-ac converter to establish the power flow through the load/grid via an ac bus. The ac-coupled topology is shown in Fig. 2(b). This topology requires two dc-ac power converter stages that are directly tied to the ac bus to connect with the load and an ac grid. In this topology, bidirectional power flow between the ac grid and the dc BES system is possible. The ac-coupled topology in shown in Fig. 2(c). It is technically similar to Fig. 2(b). The difference is that an ac BES system is directly connected to the ac bus and has a built-in inverter. This is presented here as this topology is widely marketed as a packaged solution for residential customers who wish to retrofit batteries within a home with an existing solar system [16]. An integrated TPC topology is shown in Fig. 2(d), and it can provide a better interface with the complex system comprising of the PV and BES systems with the load and ac grids. It has advantages of higher system efficiency, lower cost, faster response, and compact packaging with centralized control compared with other topologies [12]. The topology could be a promising candidate for multiple RES integration [17], [18]. There are few review papers published in the literature [8], [19], and [20]. These review papers are primarily aimed at covering some topological aspects of TPC to integrate solar and energy storage systems, however, their topological variations and technical challenges to allow grid interactive operation, i.e., provision of bidirectional power flow between BES system and the grid are yet to review broadly to understand the full potential of TPC topologies. In this paper, the authors firstly provide a comprehensive review on the DC-DC TPC topologies and then extend it to their variants, and technical challenges to implement a bidirectional ac output port.

The major contribution of this comprehensive review is to supplement knowledge gaps of the existing reviews and extend the concepts of TPC topologies for grid interactive

applications with a particular focus to implement a bidirectional ac output port to allow bidirectional power flow between the BES system and the grid. This review reveals that the bidirectional power flow between the BES system and grid can be achieved by making one of the ports of the TPC a bidirectional ac port. There are two approaches to realizing the ac port. The direct approach is to produce a topology that inherently offers a four-quadrant port. Alternatively, the ac port can be realized by combining a two-quadrant, bidirectional dc port with an inverter stage which may or may not be isolated. Both approaches are considered in this review. Firstly, this paper concentrates on a comprehensive review of the DC-DC TPC topologies expounded in recent publications for off-grid and grid-integrated systems. Secondly, this paper focus on a systematic review on the converter topologies with an ac port. A wide range of TPC topologies [14], [15], [21], [28] have been proposed for PV-BES applications. Depending on the electrical connection among the three ports, the existing TPC topologies can be categorized into three basic categories, namely non-isolated TPCs, partly isolated TPCs, and fully isolated TPCs [12]. However, it is important to further explore each of these topological variants to uncover the full range of benefits and limitations of these TPCs. The key aspect of this paper is that it covers these TPC topologies that are derived from a wide range of generic converter topologies including half bridge converters, interleaved half-bridge converters, full bridge converters, the buck, boost, and buck-boost converters, Cuk converters, sepic converters, zeta converters, forward converters, flyback converters, LLC and dual active bridge converters. It also provides a systematic comparison of each variant with quantitative analysis and identifies the favorable features of each topological variant as a sound foundation for future TPC applications. The paper is organized as follows. In Section II, the PV-BES integrated TPC topology and its power flow modes are presented. Section III discusses the reported TPC topologies. Section IV presents a detailed discussion on the reported TPC topologies. Section V presents the converter topologies with an ac port. A performance comparison of the TPC topologies with quantitative analysis is provided in Section VI. Finally, Section VII concludes the paper with details of the future research directions.

II. PV-BES INTEGRATED TPC TOPOLOGY

The schematic of the PV-BES integrated TPC topology is shown in Fig. 3. This topology has three ports where port 1 connects the PV array and two bidirectional ports connect the load and battery respectively. For analysis of the PCS, a lossless power equation [29] is considered as below, where $P_{PV}(t)$ is PV instantaneous output power, $P_{BES}(t)$ is BES charging power and $P_{ac}(t)$ is instantaneous output power.

$$P_{PV}(t) = P_{BES}(t) + P_{ac}(t) \tag{1}$$

The power flow diagram of the PV-BES integrated TPC is presented in Fig. 4. In mode I, the PV array satisfies the load demand and surplus PV generation is stored at the BES

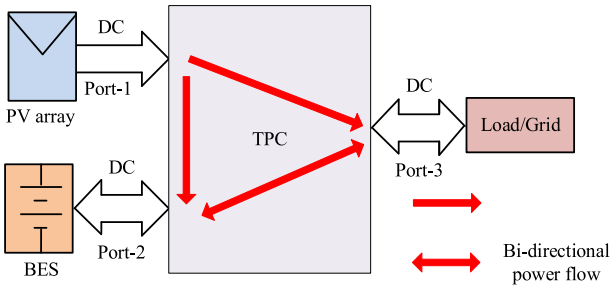

FIGURE 3. Schematic of the PV-BES integrated TPC topology [30].

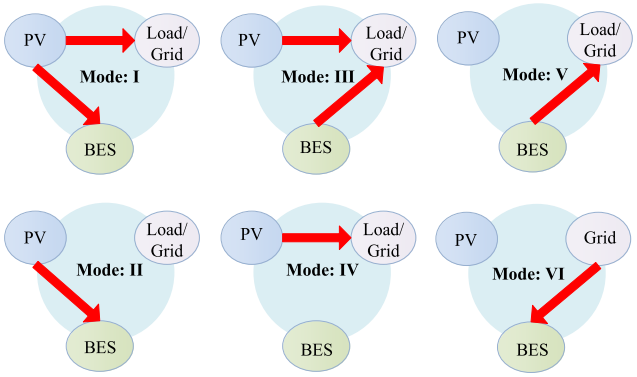

FIGURE 4. Power flow diagram of PV-BES integrated TPC topology [31].

system. In mode II, the BES system absorbs full PV power when load power demand $P_{ac}(t)$ falls to zero. In mode III, the PV array and BES provide load power demand. If the BES system charging power $P_{BES}(t)$ falls to zero, the PV array supplies power to meet load demand in mode IV. Mode V allows the BES system to meet load power demand and/or charge using grid power when PV generation is unavailable.

Mode VI allows the BES system to charge from grid while PV supplies power to the load. Operational modes V and VI require the TPC converter topology to have an ac output port capable of ensuring full four-quadrant ac operation to facilitate bidirectional ac power flow between the grid and battery [32]. The review is dominated by the TPC with three dc ports. An ac port is extremely rare. A bidirectional dc port can supply a non-isolated inverter to form an effective four quadrant ac port. The first part of this review will focus on TPCs with dc ports that can support this arrangement. TPCs with a direct ac port will also be examined.

III. REPORTED TPC TOPOLOGIES

Due to the many topological benefits of an integrated TPC over the conventional two converters for PV-BES systems, extensive research on TPC topologies is conducted and many topologies are proposed for the standalone and grid-connected renewable power systems. Most of the current literature on TPCs are concentrated on the standalone renewable power systems and very few of them are applied to grid-connected power systems. Depending on the electrical

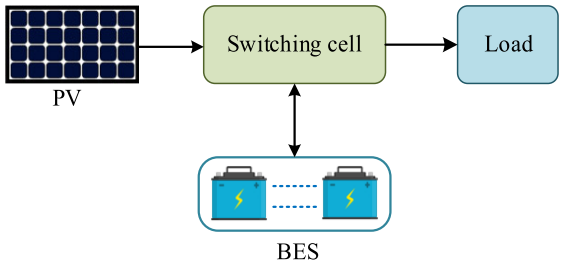

FIGURE 5. The basic structure of a non-isolated TPC topology.

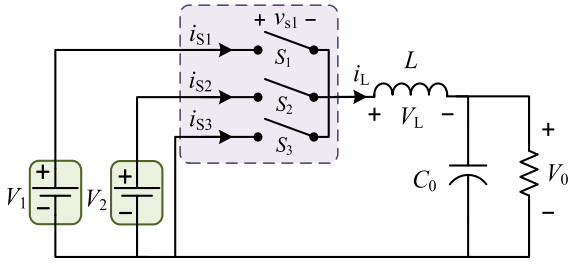

FIGURE 6. Topology based on time-sharing concept [46].

connection among the three ports, the existing reported TPC topologies can be categorized into three basic topologies [12], namely non-isolated TPCs, partly isolated TPCs and fully isolated TPCs. However, in addition to the isolation feature, these TPC topologies are further reviewed and analyzed based on their topological structure and operational characteristics such as the time-division concept, shared bus concept, single inductor concept and combining multiple generic converter concepts, etc., in the following sections.

A. NON-ISOLATED TPC TOPOLOGIES

Fig. 5 shows the basic structure of a non-isolated TPC topology where all of the ports of the TPC are connected directly without any galvanic isolation. Several non-isolated TPC topologies have been proposed in the current literature [21], [33], [44], [45], [46], [47], [48], [49], [50], [51], [52], [53], [54], [55]. These topologies can be further divided into variants based on topological structures. Fig. 6 shows a double input dc-dc converter which is derived using a single pole triple trough switch (SPST) for multiple DER applications [46]. The operation of this topology is controlled by the time-sharing concept of the active switches which entails that one, and only one, of the three SPST switches is on at any given time. When SPST switch S_1 is turned on, source V_1 delivers power to load whereas V_2 delivers power to load only when switch S_2 is on. Switch S_3 is used for freewheeling operation. With different switch realization, the topology can be configured to work on buck, boost and buck boost modes. The bidirectional power flow can be achieved by using four quadrant switches. Based on this time division concept, a multiple-input dc-dc converter [45] and a multiinput multioutput dc-dc converter [47] are proposed for EVs and other renewable energy sources. Based on the time-sharing approach and switch configurations, these topologies can be operated in buck, boost and buck-boost modes.

Depending on the power flows, the concept of the dual input converter (DIC) and dual output converter (DOC) are adopted for derivation of non-isolated TPC topologies using a single inductor (SI) with multiple switches [33], [34], [37], [48], [56], [57], [58], [59]. Many of the non-isolated TPC has single quadrant output port (SQOP) and these are topologically limited to provide single quadrant operation for the output port. The six elementary dc-dc converters, namely buck, boost, buck-boost, Cuk, zeta and sepic could be useful

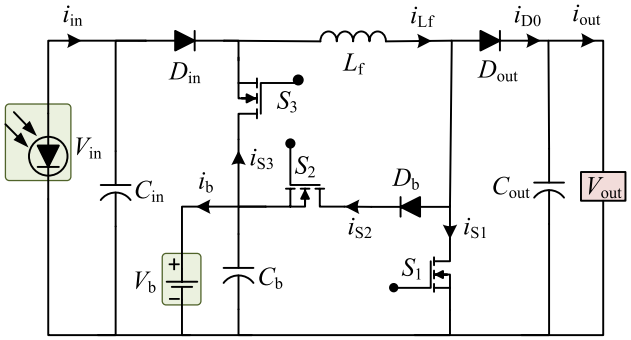

FIGURE 7. Topology based on single inductor multiple switches [37].

with the existing DOC and DIC topologies [60], [61] to provide a new energy transfer path to construct an isolated PWM TPC. A TPC topology based on single inductor with multiple switches [37] is shown in Fig. 7. The control degrees of freedom are not fully utilized in [37] and [62] and some desirable power flows are therefore missing. A similar topology is proposed using a single inductor with three switches and diodes in [48].

A family of buck, boost and buck-boost derived low cost, low power, compact non-isolated TPC topologies are proposed in [56] and [57] based on a simple and general cell consisting of two switches, two diodes. a BES system and an inductor. The four maximum control freedoms of choice for energy management between three ports are available through the two switches which extend the power flow capability of the TPC topology in [57]. This topology is fully functional in the DO and DI modes without the port voltage restrictions, unlike the topology proposed in [37] where there exists the port voltage restriction among the ports for these modes. In addition, this topology provides an additional SISO mode of operation where the PV can charge the battery only when the load requirement is idle which does not exist in [37]. The dynamics of these buck/boost/buck-boost derived single inductor TPCs (SI-TPCs) becomes complicated because of the various energy transfer modes within the multiport arrangement [44]. The differing modes result in different small signal models. A TPC topology proposed in [33] which is quite similar to the structures proposed in [56] and [57] with some additional components and the output port is also single quadrant type. As the solar and battery

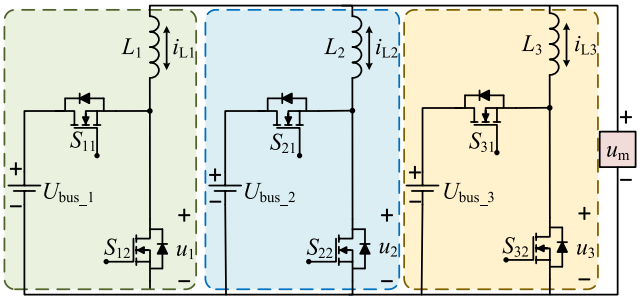

FIGURE 8. Topology based on shared bus concept [50].

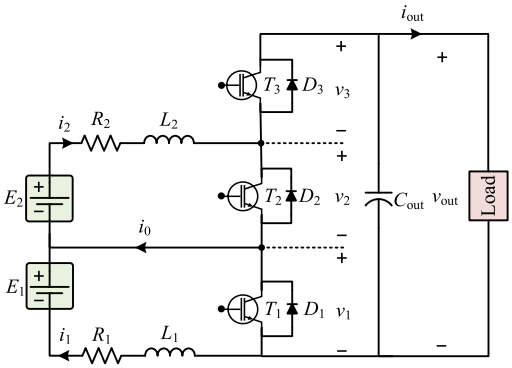

FIGURE 9. Topology based on double boost converter [51].

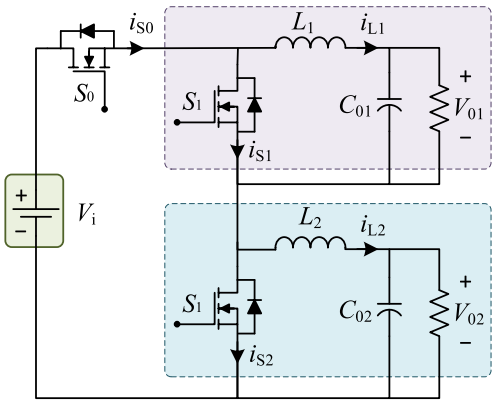

FIGURE 10. Topology based on multiple buck converter [52].

systems must operate over an extended voltage range, the major challenge with the non-isolated TPC derived from the basic buck/boost/buck-boost topology is to keep the port voltages within a suitable operating range to maintain its functionality. A compact non-isolated TPC with a reduced number of semiconductors and a common ground is proposed in [63] to address EMI issues where all three ports are grounded. This topology is based on the single inductor dual output (SIDO) converter [58], [59]. In this topology, a bidirectional path is established for the battery port, however, the output port still provides single quadrant operation. A non-isolated TPC topology is proposed based on a shared bus concept [50] as shown in Fig. 8. In this topology, the inductors form the dc-links. It provides a great improvement compared with the traditional common dc-bus-based solution as the bulky dc-link capacitor is eliminated. The topology can be realized as a three port bidirectional buck boost converter, and this provides single-stage conversion between any two of the three dc-buses. A similar shared bus concept is used to develop a modular multiple-input bidirectional dc-dc converter [49] to integrate multiple DERs at different voltage levels. The topology can be operated either in buck mode or boost mode and bidirectional power flow can be achieved. The total power required from the auxiliary sources can be shared between the battery system and the ultracapacitor bank. The power sharing is based on operating conditions such as charging current limitations and state of charge of the BES system and overall dynamics of the converter.

A family of TPC topologies are derived by combining two or more generic power converters in [40], [51], [52], [53], [54], and [55]. Fig. 9 shows a new bidirectional dc-dc boost converter topology based on double boost converters [51]. The topology is very simple, and it requires three controllable power switches and two inductors. A similar approach is used to develop an integrated single input multiple output converter using a few boost converters in [55]. The topology provides one high step-up and multiple step-down outputs at different voltage levels utilizing a lower number of switches compared to separate converters. This topology is more reliable due to its inherent shoot through protection and shows similar dynamic behavior as individual buck and boost converters. A similar concept is applied to propose a new dc-dc boost converter topology for mobile device applications [54]. A TPC topology is proposed in [40] by integrating a buck-boost converter with a stacked dual half-bridge converter. This topology provides a low and a high voltage output at the output ports and both ports are bidirectional. Fig. 10 shows a TPC topology based on multiple buck converters for EV applications [52]. The topology provides multiple regulated outputs at different voltage levels. This topology requires a reduced number of switching components compared with the conventional separate buck converters. The dynamic behavior of this integrated topology is similar to the conventional buck converter which makes the controller design relatively simple.

Based on the concept of combining multiple dc-dc buck converters to develop a multioutput topology, a TPC topology is proposed for providing dual outputs with simultaneous bidirectional and unidirectional characteristics in [53]. One of the limitations of this topology is that it requires semiconductor power switches with current ratings higher than that required in the conventional solution comprised of two separate dc-dc buck converters.

A family of TPC topologies are proposed utilizing coupled inductor in [36], [38], and [43] as a voltage gain extension cell. Fig. 11 shows the TPC topology based on coupled inductors proposed in [38] and [43]. This topology provides voltage boosting for high step-up applications and the output port is bidirectional. The topological structure of the TPC proposed in [36] is quite similar to the topology proposed in [38] and

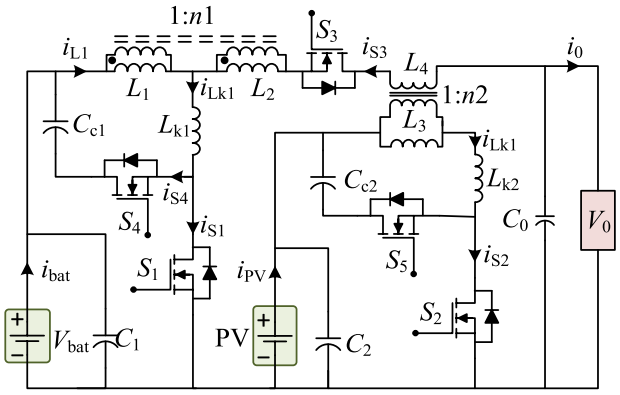

FIGURE 11. Topology based on coupled inductors [38], [43].

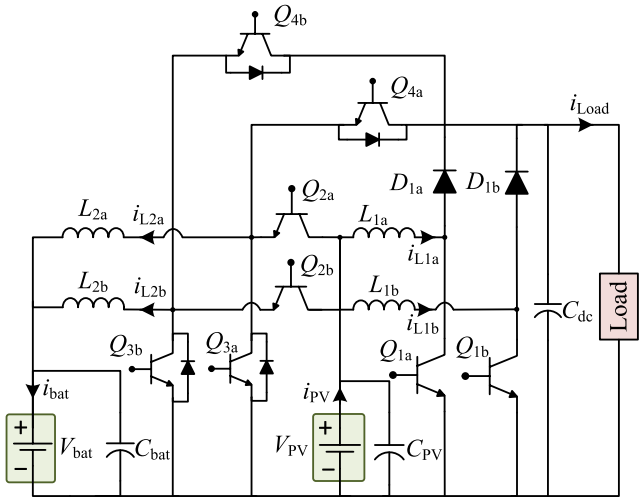

FIGURE 12. Topology based on interleaved converters [39].

[43] except the output port which is single quadrant in [36]. Like the topology in [38] and [43], this topology adopts the use of a coupled inductor to achieve a higher voltage ratio by adjusting its turns ratio. Unlike the topology in [38] and [43] that utilized complex two clamping circuits for recycling the leakage inductance energy, a lossless snubber circuit is used for the same purpose. However, this TPC topology is designed to work in DO, DI and SISO modes and the full control freedoms are also not utilized here. This structure is less complex than [38] and [43] and can achieve a higher overall efficiency within the operational modes.

A non-isolated dc-dc TPC topology based interleaved converter is proposed in [39]. The topology is derived from conventional buck and boost converters. The topology allows modular design for high power applications by interleaving multiple converter stages. Fig. 12 shows thee two stages interleaved topology that provides bidirectional power flow between the output port and battery port.

B. PARTLY ISOLATED TPC TOPOLOGIES

The general structure of a partly isolated TPC topology is presented in Fig. 13 where two ports share a common ground and are isolated from the remaining port. The isolation is

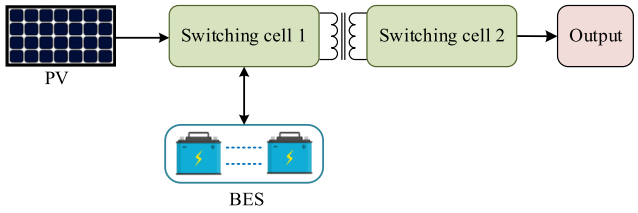

FIGURE 13. The basic structure of a partly isolated TPC topology.

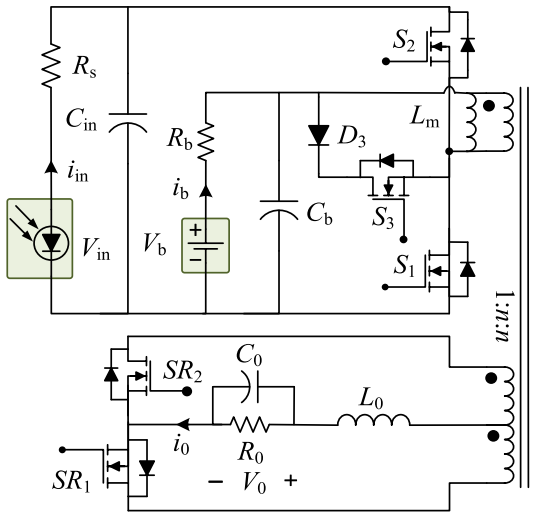

FIGURE 14. Topology based on half bridge converter with synchronous rectification [64].

generally provided by a high-frequency transformer. The partially isolated TPC can be derived with the combination of a two-port isolated converter and a two-port non-isolated converter. A group of partly isolated dc-dc TPC topologies are found in the current literature [14], [23], [29], [64], [72] using half-bridge converters [14], [64], [65], full bridge converters and DAB [23], [29], [66], [68], [70], [73], and LLC and LCL resonant converters [69], [71], [74], [75].

Partly isolated TPC topologies based on half bridge converter with synchronous rectification are proposed in [64], [65], and [67]. Fig. 14 shows the topology proposed in [64] for satellite applications where the output load port is single quadrant and is isolated from the PV and battery port by a HF transformer.

This converter is PWM modulated, however, the detailed analysis of the soft switching operation with synchronous rectification is not provided. Similar to this concept, a family of basic half-bridge converter based TPC topologies with post regulation, synchronous rectification and primary freewheeling with various implementations are proposed in [65]. This regulation is required to introduce an additional control degree of freedom to independently regulate the voltage of any two of the three ports of the TPC while the third one is used for power balance. A group of partly isolated TPC topologies are proposed in [14], [23], [29], [68], and [70] based on interleaved bidirectional half bridge converters and a secondary side bridge rectifier/converter.

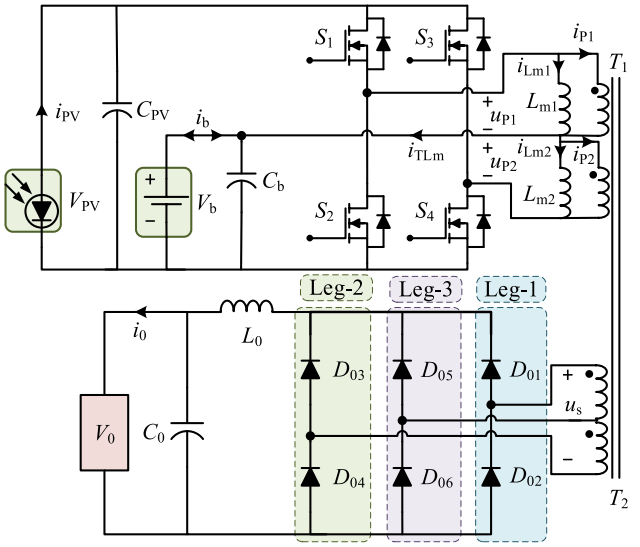

FIGURE 15. Topology based on interleaved half bridge converters and a bridge rectifier [14].

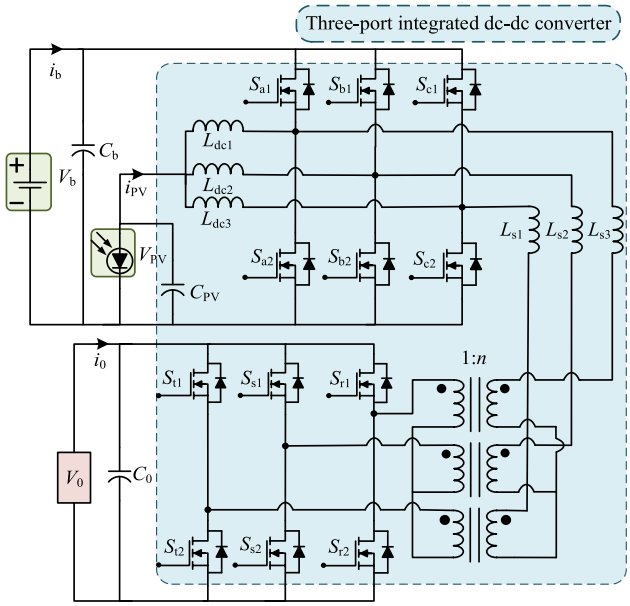

FIGURE 16. Topology based on interleaved converter and DAB [66].

Fig. 15 shows a partly isolated TPC topology based on an interleaved converter and a secondary side bridge rectifier [14]. In these topologies, the primary side bidirectional interleaved converter is PWM modulated whereas the secondary side bridge rectifier/converter is phase shift modulated. These topologies are very effective in reducing the circulating current at the freewheeling stage and extending the soft switching range of the power switches. A bridgeless boost converter is used in the secondary side to reduce the input current ripple because of the 180° phase shift between the input side switching legs in [70].

The TPC proposed in [23] and [68] are topologically the same except for an ac inductor and two diodes in [23] replacing the two power switches in the secondary side in [68]. The ac inductor further limits the circulating current at the freewheeling stage in the secondary side of the circuit as there are no dc inductors at the output circuits.

An interleaved bidirectional PWM converter is combined with a DAB converter to develop partly isolated TPC topologies in [66] and [73]. Fig. 16 shows the partly isolated TPC topology that consists of an interleaved PWM converter and a three-phase DAB converter.

The three-phase Y-Y connected transformer is used to allow bidirectional power flows with galvanic isolation and voltage matching between the different ports. A similar approach is used to develop a partly isolated TPC for EV battery systems in [73].

In this topology, a flying capacitor is added to the interleaved PWM converter to achieve the automatic current balancing for inductors in the PWM converter, eliminating an active current balancing control loop using current sensors. Furthermore, the added FC allows the MPC to operate with a nominal duty cycle of 0.5, improving the transformer utilization and reducing rms current.

Some partly isolated TPC topologies are proposed in [69], [71], and [75] based on an interleaved bidirectional buck/boost converter and a full bridge LLC resonant converter in the primary side combined with a bridge rectifier in the secondary side.

These topologies feature low power component amounts, and a simple and symmetrical structure. These topologies inherently provide high power density, low circulating currents and zero voltage switching (ZVS) operation of all the primary side switches while ensuring the turn off with zero current switching (ZCS) operation of all diodes in the secondary side for the entire voltage and power range, leading to significantly reduced switching losses.

This is very helpful for high frequency operation. The power flows of these topologies are managed by PWM and PFM approaches. Fig. 17 shows the partly isolated TPC topology proposed in [71]. Fig. 18 shows a new LCL based partially isolated TPC proposed in [74] and [76]. It features a smaller number of power switches than [69] and [71].

The output port of the aforementioned partly isolated topologies is single quadrant; however, the output side could be redesigned to have bidirectional power flow using four quadrant power switches.

C. FULLY ISOLATED TOPOLOGIES

Fig. 19 shows the general structure of a fully isolated magnetically coupled TPC topology where the three ports are fully isolated from each other. A high-frequency transformer is normally used to provide isolation between the three ports. Several fully isolated TPC topologies are proposed in the current literature [12], [24], [26], [77], [87]. The fully isolated TPC topologies proposed in [25], [77], [81], and [85] are based on the DAB converter [88]. These TPC topologies

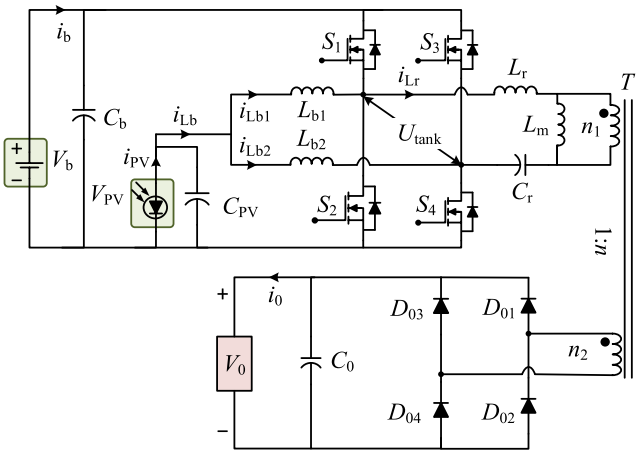

FIGURE 17. Topology based on interleaved bidirectional converter and full bridge LLC resonant converter [71].

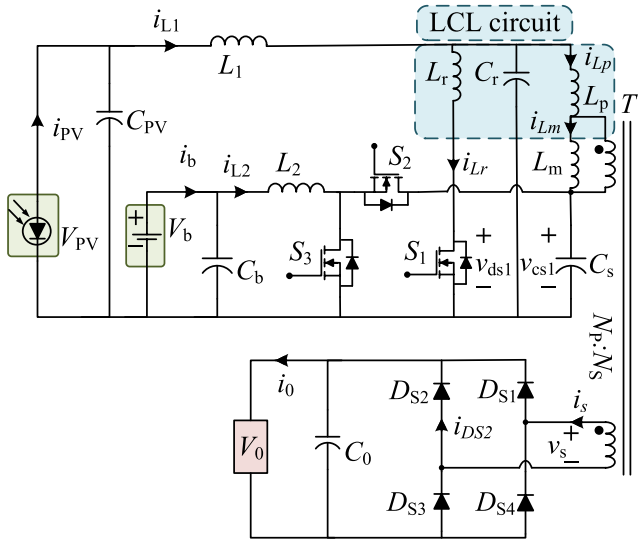

FIGURE 18. Topology based on interleaved bidirectional converter and LCL resonant circuit [74].

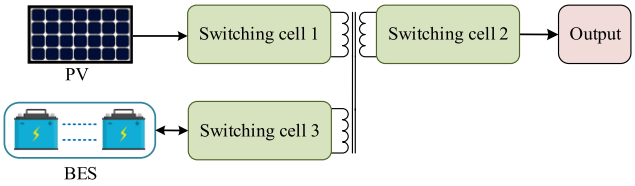

FIGURE 19. Basic structure of a fully isolated TPC topology.

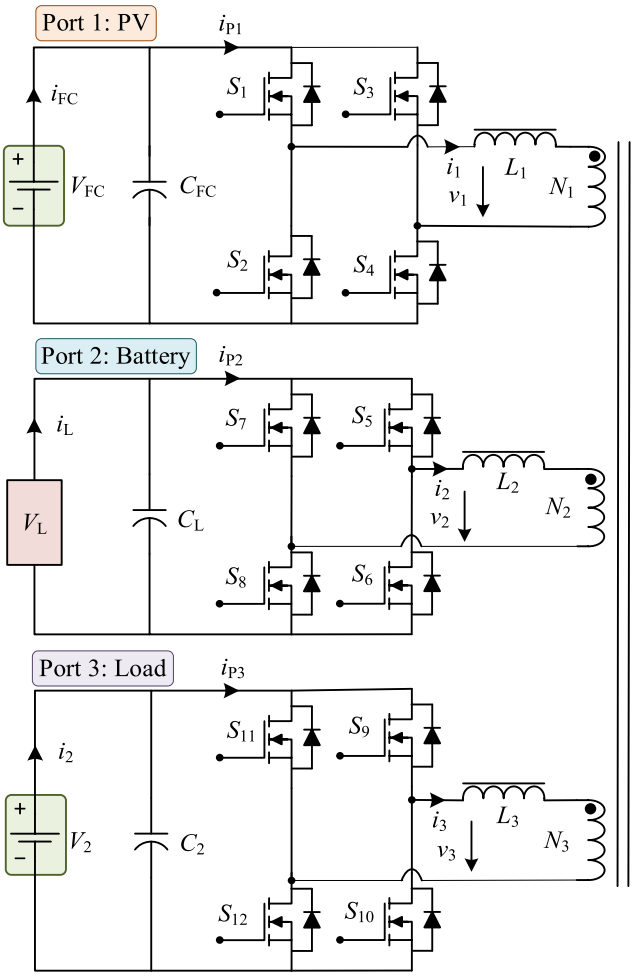

FIGURE 20. Topology based on DAB converter [25].

based on DAB converters produce triple active bridge (TAB) converters and each TAB converter consists of three full bridge converters.

Fig. 20 shows a fully isolated TPC topology based on the DAB structure [25]. There are no topological differences in the TPC proposed in [81] and [85] compared with [25] and [88]; however, a shell-type planar HF transformer in [81] and a three-limb HF transformer in [85] are used as power transfer elements among the ports to analyze the performance of these transformers and providing soft switching operation. The TAB converters have advantages such as low device stress, bidirectional power flow capability, and fixed frequency operation.

The TAB converters are used for grid connected renewable energy systems in [84]. The topology is the same as the topologies proposed in [25] and [77], however, an additional converter stage with LCL filter is connected to the dc-link at the output port to interface with the grid. A similar TAB converter topology is proposed in [79] for EV charging systems. An extra full bridge diode rectifier is connected with the active bridge in the EV charger port via a dc-link to interface with the grid [79]. An integrated fully isolated TPC topology based on a TAB converter is proposed in [86]. However, in this topology, two three-winding transformers and four full-bridges are utilized to establish all five possible power flows. In the output port, two isolated full bridges are connected in series for boost operation. The secondary windings are connected in a special way. The TAB converter is used to develop an isolated series resonant TPC topology in

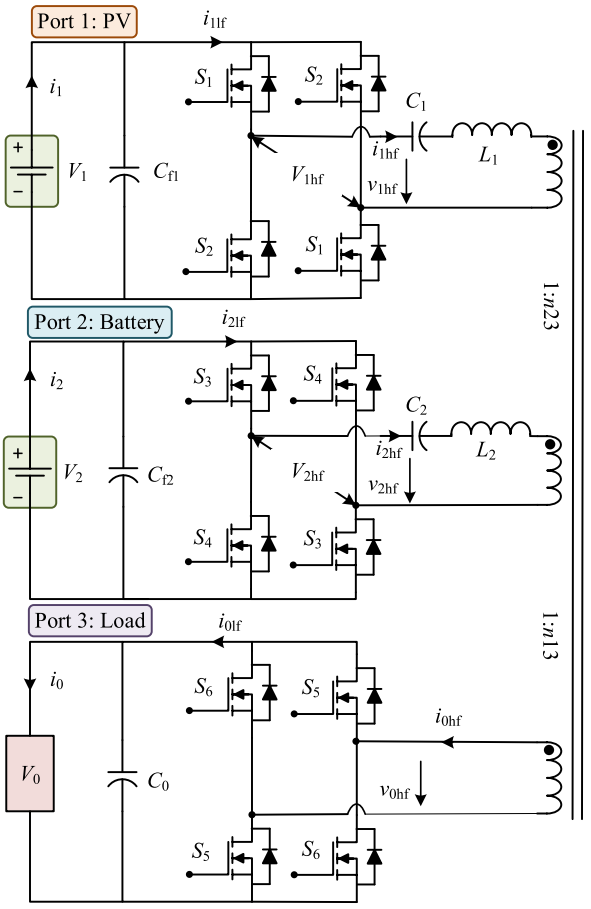

FIGURE 21. Topology based on series resonant DAB converter [26].

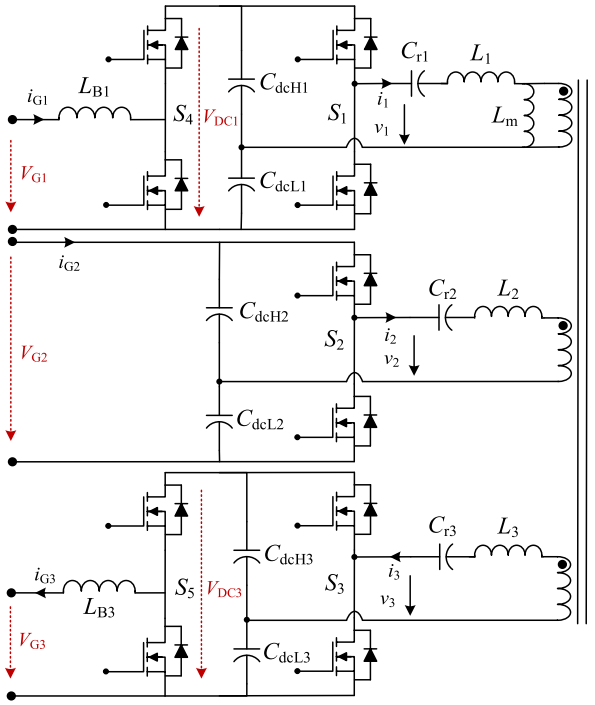

FIGURE 22. Topology based on three-half bridge with a three winding transformer and LLC resonant circuits [24].

[26] and [78]. Fig. 21 shows a series resonant isolated TPC topology proposed in [26]. In this topology, the input side bridges are connected by a series LC resonant circuit. In [78], the load port consists of a full bridge diode rectifier and thus it cannot handle bidirectional power flow. An isolated LLC resonant dc-dc TPC for DC applications is proposed in [24] as shown in Fig. 22.

In the inner stage, three half bridges are connected with a three winding MF transformer through an LLC resonant stage, making a symmetrical LLC resonant converter. In the outer stage, additional buck/boost stages are connected at port 1 and port 3 for achieving the active power flow control.

IV. DISCUSSION ON REPORTED TPC TOPOLOGIES

In this paper, the reported TPC topologies are grouped into three different categories based on their isolation arrangements namely non-isolated TPC, partly isolated TPC and fully isolated TPC. Further to this classification, each of these TPC topologies are individually analyzed and further subdivided into various topological variants based on their circuit configurations and operations. The key parameters such as power ratings, voltage levels at the ports, component counts, operating frequency and efficiencies of non-isolated, partly isolated and fully isolated TPC topologies are presented in Tables 1, 2, and 3 respectively to explore the pros and cons of these TPC topologies. This section focuses on important features of the individual categories that will form a very useful reference for future TPC design and implementation.

A. NON-ISOLATED TPC

A non-isolated TPC is generally derived from the basic converters, i.e., buck, boost, and buck-boost, that share switches and storage elements in each switching cycle [22]. The advantage of this type of topology is that it is smaller in size and weight due to the absence of a transformer for electrical isolation. This topology also offers high power density, high efficiency and high reliability due to lower component counts. Table 1 shows the details of the key parameters for the non-isolated TPC topologies. However, there are few major drawbacks as follow:

1) PORT VOLTAGE RESTRICTIONS

As these topologies are transformerless, they suffer from limitations on port voltage ranges when dealing with sources like PV and BES system that exhibit a wide voltage variation under certain conditions [15]. For example, the non-isolated topology proposed in [35] operates normally only when the PV and battery port voltages are higher than the load voltage.

2) VOLTAGE GAIN

In some power flows, the voltage gain of the non-isolated TPC becomes similar to the conventional boost converter that

TABLE 1. Key Parameters of Reported Non-isolated Topologies.

Refs	Rated power (W)	Input Port 1/ PV Voltage (V)	Input Port 2/ Battery Voltage (V)	Output Port/Load Voltage (V)	Power Switches and Diodes	Switching Frequency (kHz)	Inductor (uH)	Capacitors (uF)	Bi-directional ports	Average Efficiency (%)
[45]	-	5	10	7	8	50	50	680	Yes, BES	-
[46]	550	80	60	50.5	5	50	50	150	Yes, BES	89
[47]	220	35	48	120	8	10	2000	2@1000		80.50
[48]	120	24	36	48	6	100	100	2@1000		83.6
[37]	1000	35-70	70-100	100	6	100	50	-	No	96.5
[49]	5000	125-144	120	300	6	20	2@750	3000	Yes, BES	92.5
[50]	1000	90-110	90-110	90-110	6	100	3@25	3@200	Yes, BES	98
[51]	-	96	42	400	3	20	2@100	10000	Yes, BES	90
[91]	240	60	24	48	4	100	47, 100	9@68, 2@4.7, 17@10	BES	96
[52]	~100	48	-	12, 5	3	100	75, 47	2@220	No	90
[53]	-	100	-	40, 20	3	50	2@2000	2@2200	Yes, BES	-
[54]	4	2.4	3.5	4.0	3	100	2@47	3@100	Yes, BES	93
[55]	120	12	-	18, 6	3	100	15, 10	550, 220	No	90
[57], [44]	24	18	24	12	4	20	-	-	Yes, BES	-
[38], [43]	200	52.8	48	380	5	50	2@1, 2@52	1@47, 2@470	Yes, BES	90.1 max at 110W
[36]	300	24	48	400	7	50	-	-	Yes, BES	94
[39]	4000	200-500	150	600	5	20	1000, 800	35	Yes, BES	97 (SiC diodes)
[40]	1000	-	30-42	72, 400	4	100	15.63, 30.29	4@ ---	Yes, BES	97
[33]	120	10-50	36	24	6	20	62	-	Yes, BES	93.5
[92]	200	0-150V	24	60	3	20	333, 833, 480	3@680	Yes, BES	90
[93]	80	18	12	50	4	50	100, 400	2@470	BES	93.7
[94]	120	30	12	220	10	25	660, 980	3@220, 120	BES	94.5
[95]	200	24	36	380	5	30	600, 60, 4800	2@15, 47,150	BES	94.3
[96]	250	60	96	200	10	100	479	10	BES	96
[97]	100	0-360	24	750 (max)	5	50	2@184	100, 120, 180	BES, Load	93.4
[98]	250	48	24	200	8	50	200	2@120	BES	96.3

increases the voltage stress on the semiconductor switches. For example, the voltage gain of the TPC is the same as the boost converter when the TPC operates in dual output and dual input modes [37].

3) SINGLE QUADRANT OPERATION

The output ports of the non-isolated TPC topologies are frequently limited to single quadrant operations. These topologies are predominantly designed to have unidirectional diodes at the output ports. In some cases, output ports of these converter topologies could be made bidirectional using bilateral inversion techniques [89] that allow unidirectional diodes to be replaced with bidirectional active switches.

4) COMPLEXITY OF ACHIEVING FOUR QUADRANT OPERATION

None of the non-isolated TPCs have a four-quadrant port. The extension of the output port to four-quadrants requires a voltage reversal capability and this is not normally feasible as the impacts propagate to all ports given the absence of an isolation boundary.

5) OTHER COMPLEXITIES

To alleviate the port voltage restriction problems seen among the ports in [37], [56], and [57], a non-isolated TPC with variable structures can be used [15]. However, the trade-off could be a higher component count, higher cost and lower reliability. To reduce the voltage stress of the semiconductor devices, coupled inductors can be used as a voltage gain extension cell [38]. However, a problem with many coupled inductor designs is leakage inductance. The leakage inductance energy must be managed to maintain the converter efficiency and to limit device switching stresses. The non-isolated topologies may be applicable for relatively low power application where there is no need for isolation to comply with safety requirements [90].

B. PARTLY ISOLATED TPC

Amongst the three TPC topologies, the partly isolated topology has received the greatest interest and many of these topologies are available in the current literature. Partly isolated TPCs normally have isolation for the load port while PV and battery ports are connected via buck, boost or buck-boost converters that share common switches [14]. The partly isolated topology removes the port voltage restriction at the load port. However, the partly isolated TPC topology has the following shortcomings:

1) COMPONENT COUNT

This topology has a higher component count as compared to the non-isolated TPC topologies and the problem of port voltage matching will still appear at PV and battery ports.

TABLE 2. Key Parameters of Reported Partly-isolated Topologies.

Refs	Rated power (W)	Input Port 1/ PV Voltage (V)	Input Port 2/ Battery Voltage (V)	Output Port/Load Voltage (V)	Power Switches and Diodes	Switching frequency (kHz)	Inductor (uH)	Capacitors (uF)	Bi-directional ports	Average Efficiency (%)
[64]	200	60	28	28	6	20	65, 45	2@680, 210	Yes, BES	-
[65]	120	25-35	10.5-13.5	25	4	100	66, 85	2@330, 100	Yes, BES	-
[14]	500	60-80	30-42	100	10	100	100, 200	-	Yes, BES	94.5
[29]	300	38-76	26-38	42	8	100	100, 70	3@470	Yes, BES	92
[66]	3000	32-48	67.5	270	12	40	7.5, 1	5600, 780	Yes, BES	-
[68]	600	30-50	64-80	100	8	100	2@100, 5	-	Yes, BES	95
[70]	500	70-100	42	300	8	100	2@35, 20		Yes, BES	96
[23]	1000	25-60	120	300-380	8	60	2@155, 28	4@20, 3@22	Yes, BES	95
[71]	500	65-115	165-200	360	8	74-100	-	-	Yes, BES	-
[69]	500	65-115	165-200	360	8	74-100	2@150, 34.5	73.5 nF	Yes, BES	95
[74]	120	22	7.5	50	7	100-170	2@320, 75, 2@3.3	4@1000, 0.22	Yes, BES	93.5
[67]	~120	43.2	24	180	5	200	320, 18	2@110, 220	Yes, BES	-
[73]	1000	54	14	250	8	50	2@15	10, 100. 200, 300, 180	Yes, BES	94
[75]		70-130	96	380	18	200	30, 70, 2@0.7, 1.0	600 nF	Yes, BES	93.7

2) COMPLEXITY WITH TOPOLOGICAL VARIATIONS

Partly-isolated TPC topologies using basic half bridge converters are simple and provide high power density. However, the switching losses are high because of the hard switching and high circulating currents caused by the freewheeling operation in the body diodes of the switches [99]. The power rating of these converters is also limited by the requirement for tight primary to secondary coupling. To reduce switching losses, a magnetizing inductor can be used in the design to provide the soft switching operation of the primary side switches. On the other hand, the partly isolated TPC topologies employing full-bridge structures can achieve soft switching operation and reduce the input current ripple. As the full bridge converters are controlled by a phase shift, the primary side phase shift (PSPS) based full bridge topologies with simple phase shift modulation strategy suffer from the limited soft switching operation range, high circulating current, high current ripple and the narrow voltage conversion range [66], [99], [100]. A full bridge interleaved bidirectional boost converter and a bridgeless boost rectifier based partly isolated TPC topologies reduce input current ripple; however, additional active switches are required for a phase shift to establish power flow control between ports that make driver circuit requirements more complex [70]. The body diodes of the MOSFETs experience hard switched conditions that add additional reverse recovery losses in the design [70].

LLC resonant converters can achieve ZVS and ZCS, however, much effort should be given to control the LLC converters as soft switching conditions and other parameters greatly depend on the resonant frequency. The partly isolated topologies are suitable for applications in which the low operating voltage of PV and battery need to be boosted to match the load side high voltage, which further feeds an inverter to generate an ac output.

The output ports of the majority of the partly isolated converters reviewed are topologically designed as either half bridge or full bridge configuration with output diode rectifiers. Putting aside likely impacts on switching stress or soft switching arrangements, the output ports of these converters can be potentially converted to bidirectional ports using bilateral inversion techniques [89] and replacing the diode with active switches. In some cases, and again putting switch stress issues to one side, a four-quadrant port may be possible by replacing the output diodes with four quadrant switches with bidirectional conduction and blocking ability.

C. FULLY ISOLATED TPC

The main advantage of fully isolated TPCs is that they provide independence of voltage levels at each port [82]. This style of TPC exhibits a symmetrical structure between ports that makes driving and control circuitry symmetrical for each port and thus makes the converter control issues less complex [25], [30]. The energy transfer can be established by the leakage inductor of the high-frequency transformers. In addition, the HF transformer provides full isolation and voltage matching among the different ports. However, the fully isolated full bridge structure has the following drawbacks:

1) COMPONENT COUNT

When compared with the non-isolated converters, the fully isolated structure will have a greater component count and the use of the high-frequency transformer will increase the overall size and therefore relatively reduce the power density and reliability [37].

TABLE 3. Key Parameters of Reported Fully-isolated Topologies.

Refs	Rated power (kW)	Input Port 1/ PV Voltage (V)	Input Port 2/ Battery Voltage (V)	Output Port/Load Voltage (V)	Power Switches and Diodes	Switching frequency (kHz)	Inductor (uH)	Capacitors (uF)	Bi-directional ports	Average Efficiency (%)
[77]	1.5	42	14	300	12	100	21, 495 nH, 55 nH	-	Yes, all	91
[25]	1.0	54	21-42	400	12	20	1.2. 65, 0.73	50	Yes, all	-
[84]	5.0	225	150	600	16	10	3@30	-	Yes	-
[86]	1.0	10-40	10-40	60-200	16	100	-	-	Yes	94
[26]	0.5	50	36	200	12	100	28.4, 14.7, 70	0.1, 0.22	Yes, all	91
[24]	350	3000	1500	400	10	5	10, 13.7, 2.6, 29.8	66.6, 354.1, 30.7 96.5, 555.6, 444.5, 80.5, 421.2, 31.23	Yes BES, Load	-
[105]	50	100	100	100	12	10	48.125 mH, 0.024 mH	3@330	Yes, all	98.8
[106]	150	880-1300	800-1300	1300	12 (SiC)	20	2@19, 31	3@390, 2@195	Yes, all	98.8
[107] [108] [109]	0.8	160	22	120	12 (SiC & GaN)	100	15, 16, 0.28, 300	47, 86	Yes, all	95
[110]	2.0	480	480	600	12	100	414, 319	7@15nF	Yes, all	97.75
[111]	0.5	60	60	100	8	190	24, 30, 780	60 nF	Yes, all	94
[112]	6.6	270-450	9-15	400	12	600-800	3, 19.2, 125 nH	8.8, 400, 1.98mF, 3.36mF, 8.8, 246 nF	Yes, all	94
[113]	0.3	54	48	110	15	10	6.51, 9.6, 6.67		Yes, all	93
[114]	1.0	150	120	200	12 (SiC)	50	2@600, 2@204, 101.3	2@220, 2@53, 100	Yes, all	-

2) CONDUCTION LOSSES AND ZVS RNAGE

The fully isolated TPC topologies based on a DAB/TAB with simple phase shift control cannot operate effectively under wide input voltage variation, leading to high conduction losses and a reduction of the soft switching range [101], [104].

3) RESONANT STRUCTURE

To minimize the losses, resonant TPC topologies can be used [24], [26], [78]. However, the crucial parts of these resonant TPC topologies are the design of resonant parameters. The operating point of the converter may change with the resonant frequency and the control implications associated with the resonant circuit make this topology very complex. However, these problems can be effectively alleviated by applying improved modulation and control strategies. TPC topologies based on the full bridge structure are an appropriate choice for interfacing with the ac grid and these are normally designed for relatively high power applications [25]. This requires one of the three ports of these TPCs to be bidirectional ac to allow full four-quadrant operation for grid interactive applications. Some isolated converters, such as those derived from the DAB, have a high degree of symmetry and naturally offer two quadrant ports. They are the most adaptable to four quadrant port operation through the introduction of four-quadrant switches.

V. TPC TOPOLOGIES WITH AC PORT

In Sections III and IV, the review examines a range of non-isolated, partly isolated, and fully isolated dc-dc TPC topologies and discusses the benefits and limitations of those topologies with their key parameters. In this section, the authors aim to explore the TPC topologies with a direct full four quadrant ac output port which is very essential for grid interactive PV-BES integrated systems. The review identifies different topologies such as the boost derived converter [115], [116], Z-source inverter [117], matrix converter [118], [119] and DAB with back-to-back converter that are used to implement the direct ac port which are discussed below.

A. BOOST DERIVED CONVERTER

A new TPC topology with a direct AC output port is proposed in [115]. This topology is shown in Fig. 23 which is a boost derived non-isolated converter system having two dc input ports and an output AC port. The topology consists of two switching legs where only three active switches are used for each leg. The proposed topology can support buck, boost, and ac conversions. However, the maximum modulation index for

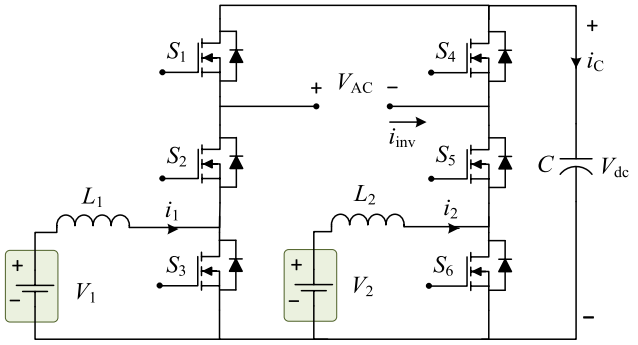

FIGURE 23. TPC topology with a direct AC port based on boost derived converter [115].

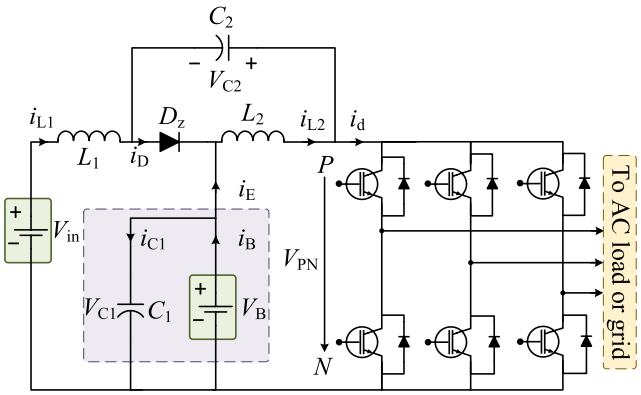

FIGURE 24. TPC topology with a direct AC port based on Z-source inverter [117].

ac conversion is limited due to the buck and boost operation of the dc/dc parts of the converters.

A similar boost-derived converter topology with a direct AC output port is proposed in [116] for residential applications with simultaneous dc and ac loads. The topology is defined as a boost-derived hybrid converter (BDHC) as it is designed from a generic boost topology and it can provide simultaneous DC and AC outputs at the output ports [116]. The BDHC topology is realized by replacing the controlled switch of single-switch boost converters with a voltage-source-inverter bridge network. This converter gives extra flexibilities to interface with one of the dc ports to supply ac loads.

B. Z-SOURCE INVERTER

Z-source inverters can also be used as TPC with a direct ac output port. A new topology of the energy stored Quasi-Z-Source Inverter (qZSI) is proposed for PV power system applications in [117]. The topology is shown in Fig. 24. The qZSI topology is capable of simultaneously controlling the inverter output power, tracking MPP and managing the battery power regardless of the charging or discharging situation. The voltage boosting and inversion, and energy storage features are integrated in the qZSI.

C. MATRIX CONVERTER

Matrix converters are gaining more attention as alternative solutions to power converters with bulky dc-link capacitors.

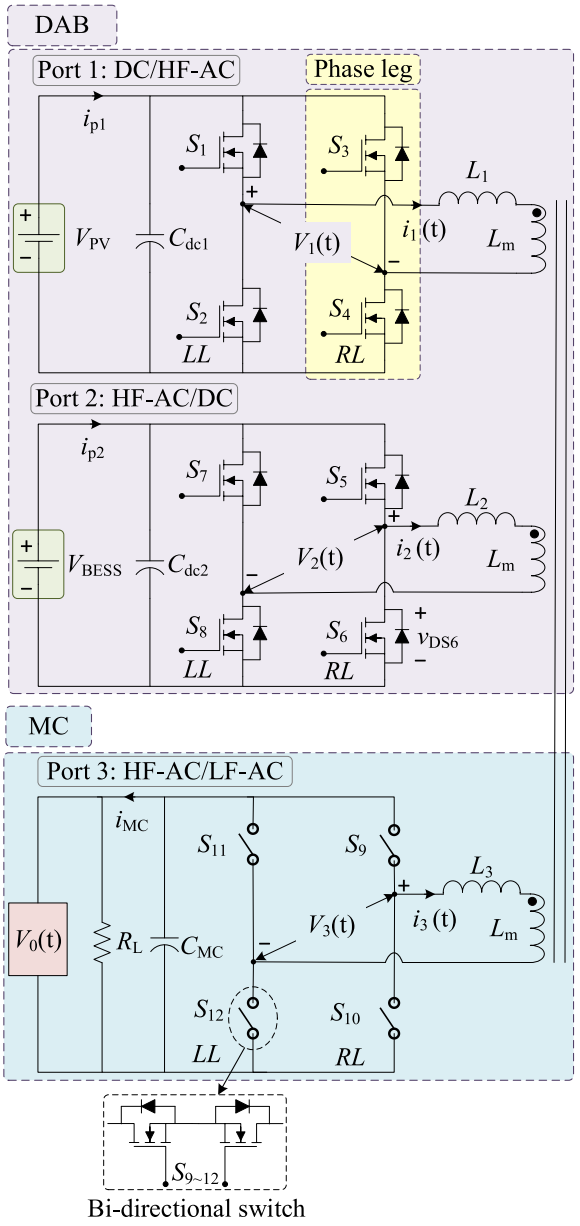

FIGURE 25. TPC topology with a direct AC port based on DAB and matrix converter [30].

The matrix converter can provide size, weight and volume advantages for grid interconnection of the microgrids, generation systems, and loads [120]. Compared to traditional converters based on rectifier-inverters, the matrix converter system also provides several technical benefits [121], [122]. The key benefit is its inherent four quadrant power flow. Therefore, in relation to a DAB converter for the PV and BES port, the matrix converter system can be used to implement a full four-quadrant bidirectional ac output port for grid integration. In this case, a full bridge converter using four bidirectional switches is integrated with the DAB converter to implement the ac output port to allow four quadrant power flows. The realized TPC topology with a direct ac port based on a DAB and matrix converter is presented in Fig. 25.

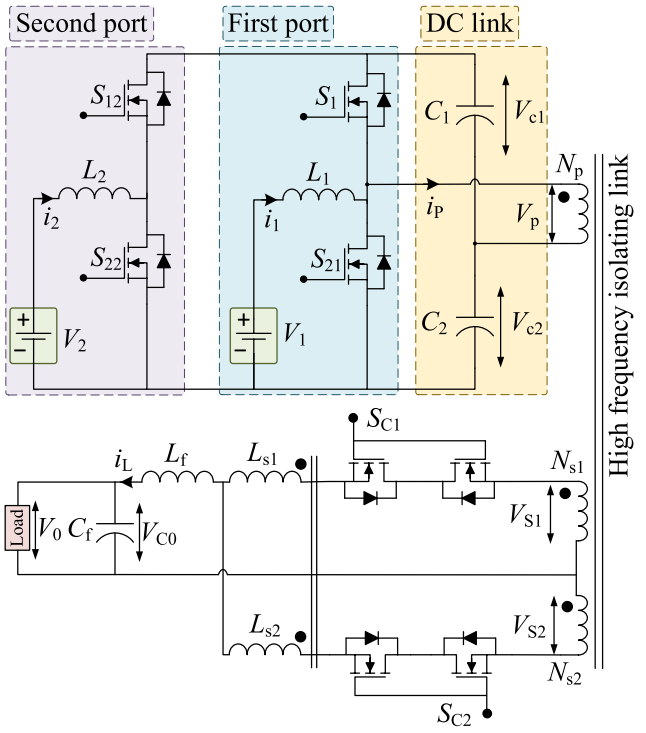

FIGURE 26. TPC topology with a direct AC port based on boost converters and a matrix converter [118].

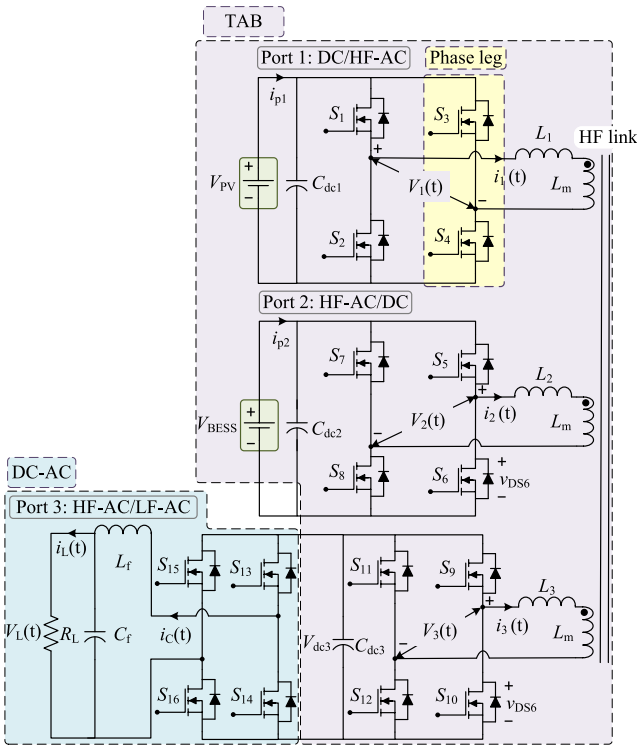

FIGURE 27. TPC topology with a direct AC port based on DAB and a back-to-back converter.

The commutation techniques and control strategies for a direct form single phase matrix converter system are challenging, specially to deal with the wide voltage range required to synthesize a low frequency sinusoidal output voltage. This requires a proper commutation method to ensure safe switching operation of the single phase matrix converter [121], [123].

A similar concept is used to implement a direct DC-AC conversion with high-frequency link in [118]. The topology is shown in Fig. 26. In this topology, the output port is realized by a matrix converter for direct dc-ac conversion and the input ports are derived from generic boost converters that can increase the dc input voltages, thus meeting the requirement of many distributed generation systems, such as PV and BES systems. The voltage boosting feature of this topology reduces the turn ratio of isolated HF link transformer. The boost inductor also reduces the input current ripple; therefore, the saturation of the HF transformer can be controlled. The component counts are reduced compared with the DAB derived topology. The topology becomes compact and that reduces the cost, size, and the volume of whole converter system.

A TPC topology with a direct ac port is proposed in [119] using an indirect matrix converter for applications in various motor drive systems including HEV. The direct dc-ac conversion is performed by an Indirect Matrix Converter (IMC) and the neutral point connection of a motor is utilized by connecting to an additional DC-DC converter. The DC link part of the IMC connects a boost-up type DC-DC converter and batteries to perform as a secondary power source to drive the motor.

D. BACK-TO-BACK CONVERTER WITH A DC-LINK CAPACITOR

In recent years, converters with non-polarized dc-link capacitors have been proposed because of size, cost and life-time advantages [124]. These could be a viable choice for the grid connected integrated PV-BES systems. The overall converter system can be developed by a triple active bridge (TAB) converter and an additional full bridge converter to connect one port to the grid as shown in Fig. 27. Therefore, the overall TPC will topologically have 16 active switches if the grid connection is single phase. However, single phase loads always produce a double frequency power ripple. This can appear on the dc-link capacitor and may propagate to the PV port [125], [127]. Consequently, the operating point of the MPPT changes due to this double frequency voltage ripple on the dc-link. There are control methods for this style of TPC topology to direct the ripple power away from the PV port. Table 4 shows the key parameters of TPC topologies having a direct AC output port.

VI. PERFORMANCE COMPARISON

The key parameters and discussion of the non-isolated, partly isolated, and fully isolated dc-dc TPC topologies along with TPC topologies having a direct AC output port are presented

TABLE 4. Key Parameters of Direct AC Port Converter Topologies.

Refs	Topology	Rated power (W)	Port 1/ PV Voltage (V)	Port 2/ Battery Voltage (V)	Output Port/Load Voltage (V)	Power Switches & Diodes	Switching Frequency (kHz)	Inductor (uH)	Capacitors (uF)	Bi-directional Ports	Average Efficiency (%)
[116]	Boost derived hybrid converter	600	48		100 (dc) 30 (ac)	5	10	5 mH, 500	1 mF, 10	No	87
[115]	Buck/Boost	~400	76 (dc bus)	12	45 (ac)	12	15	2.2mH, 3mH, 5mH	8	Yes	94
[117]	Z-source	3000	0-165	170	255 (dc)	7	20	2@500	2@400	Yes	-
[118]	Matrix converter	~140	40	30	110 (ac) 60 Hz	6	15.8	3@5, 2@10, 60	4, 2@100	Yes	-
[119]	Matrix converter	750	200 (ac) 50 Hz	100	173 (ac) 35 Hz	15	20	1.7 mF	2.5	Yes	96.5

in Sections IV and V respectively. In this section, detailed comparisons of the reviewed topologies are presented based on their topological classification. The topological mapping presented in Table 5 shows that many different types of TPC topologies can be derived by the combination of a group of generic converters such as buck, boost, buck-boost, Cuk, sepic, zeta, forward, flyback, half bridge (HB), full bridge (FB), DAB, and LLC resonant. A comparative study of these converters reveals that the peak switch current for forward, flyback and half bridge converters is double that of full bridge converters. It is also evident that the number of switches required in forward, flyback derived isolated bidirectional DC converters are less than for the half-bridge and full-bridge converters that are of six and eight switches topology respectively [82]. However, the full bridge and half bridge converters offer natural voltage clamping for the switches because of their inverse diodes and the removal of the need to depend on well coupled winding structures as found in the forward and flyback applications. In addition, because of the higher number of switches, the power capacity is largest in the full-bridge topology compared with any other of the topologies, as the power transmission capacity is proportional to the number of switches if the rated voltage and current of the switches remain the same. The transformer utilization factor for the half bridge and full bridge converter is very good, whereas the forward and flyback converters can use only half of the B-H loop, limiting the duty cycles. These advantages are such that, in higher power converters, the full bridge is nearly universally applied.

The LLC converters that operate based on the variable frequency and phase shift control modulation are very attractive and becoming popular recently for industrial and PV applications [128], [129]. The LLC converters work well as a unidirectional two-port dc-dc converter in dc-dc power conversion systems. However, their control strategies seem to be very complex for applications requiring bidirectional power flow capability with at least one bidirectional port AC due to the characteristics of LLC networks [23]. A complex control scheme is required for the half bridge, LLC and full-bridge converters. It is evident from the literature that the full bridge topology offers minimal voltage and current stresses in the devices and minimum VA rating of the high frequency transformer and low ripple current levels in the output filter capacitor [88]. At the same operating voltage, the output filter circuits are expected to be smaller for full-bridge converter as the output ripple frequency is twice the switching frequency, whereas the ripple frequency is the same as the switching frequency for forward converters. Two active switches are conducted simultaneously for the full-bridge converter during half of the switching cycle, whereas one switch is used for the forward and flyback converters. Therefore, the conduction losses would be higher for the full-bridge converters. However, the benefits of soft switching operation over a wide range, bidirectional power capability, modularity and symmetric structure of DAB [130] are attracting a lot of attention from research communities, hence DAB is expected to be one of the core circuits for high-frequency link power conversion systems [82]. From the above discussion, it is apparent that DAB derived converters are strong candidates for power conversion in PV-BES integrated systems. There are effectively two choices. A converter can be assembled using a TAB and an additional inverter stage to interface one port to the grid. An alternative is to modify one port of the TAB with four quadrant switches to gain a matrix converter functionality to allow a direct grid connection. The improved modulation and control strategies method needs to be applied to DAB/TAB converters to achieve favorable switching conditions to improve the converter efficiency and reliability. The overall size, weight, and cost of the TPC can be minimized by the sophisticated design of the HF transformer link.

VII. RECOMMENDATION AND FUTURE RESEARCH DIRECTIONS

The reported TPC topologies are categorized into three different arrangements based on isolation between the ports i.e., non-isolated topologies, partly isolated topologies and fully

TABLE 5. Comparison of Control/Hardware Limitations and Key Features for the TPC Topologies.

Refs	Topology	Power (W)	Supported Power Flow Modes	Control /Modulation methods	Hardware limitations, key features and applications
[46]	Single inductor dc-dc boost (Time-division concept)	550	IV, V	Duty Cycle Control (DCC)	• Output is unidirectional and bidirectional flow can be achieved by using four quadrant switches • Effective duty cycle and voltage gain are limited • Efficiencies tend to reduce due to increased rms currents of each input port.
[47]	Single inductor dc-dc boost (Time-division concept)	220	I, III	DCC	• Output is unidirectional and bidirectional flow can be achieved by using four quadrant switches • It is possible to have several outputs at different voltage levels.
[48]	Single inductor dc-dc boost (Time-division concept)	120	I, II, III, IV, V	DCC	• Output is unidirectional and bidirectional flow can be achieved by using four quadrant switches • It is suitable for standalone PV system applications
[96]	Single inductor bidirectional boost derived	250	I, II, III, IV, V, VI	PWM plus DCC	• Output is bidirectional • Suitable for hybrid energy systems applications
[98]	Single Coupled inductor Buck/Buck-boost	250	I, II, III, IV, V	DCC	• Output is bidirectional • Suitable for dc-dc high step-up applications
[37]	Boost (Shared bus concept)	1000	I, III, V	PWM	• Output is unidirectional • Tight port voltage regulation • Bidirectional flow can be achieved by active switches • Power sharing are possible between source and battery
[49]	Bidirectional boost (Shared bus concept)	5000	I, II, III, IV, V, VI	DCC	• Output is dc-dc bidirectional • Port voltage restrictions are partially improved/minimized • Power sharing are possible between source and battery.
[50]	Bidirectional buck-boost (Shared bus concept)	1000	I, II, III, IV, V, VI	PWM	• Output is dc-dc bidirectional • Port voltage restrictions are partially improved/minimized
[55]	Boost	120	I, II	PWM	• Dual output converter and outputs are dc-dc unidirectional • It provides a step-up and a step-down output • Compared to separate converters, this topology has lower component counts and is more reliable due to its inherent shoot through protection
[57], [44]	Single inductor buck-boost	24	I, II, III, IV, V	PWM	• Output is dc-dc unidirectional
[38], [43]	Boost (High step-up)	200	I, III, V	DCC	• Output is unidirectional • Suitable for high step-up applications • Active clamp circuits are used to improve the efficiency
[36]	High voltage gain	300	I, II, III, IV, V	DCC	• Output is unidirectional • Two input sources share only one inductor which reduces the volume of the converter
[39]	Interleaved buck-boost	4000	I, II, III, IV, V, VI	DCC	• Output is bidirectional • It is modular design and power rating is increased by means of interleaving techniques. • It is suitable for high efficiency integrated PV and BES systems where no galvanic isolation is required
[40]	Stacked Dual half bridge	1000	I, II, III, IV, V, VI	PWM plus PS	• Output is bidirectional • It is simple structure and provides high integration with smaller size and weight. • It is suitable for DC distributed power system and can be applied in DC microgrid
[33]	Variable structure	120	I, II, III, IV, V	PWM	• It possesses very tight Port voltage restriction • It is suitable for low power applications where there is no need of galvanic isolation
[92]	Reconfigurable structure (Cuk)	200	I, II, III, IV, V, VI	DCC	• Output is bidirectional • Based on Cuk converter
[93]	Reconfigurable structure (buck, buck-boost, forward)	80	I, II, III, IV, V	PWM	• Output is unidirectional
[91]	Combining two dc-dc converters (buck derived or boost derived)	240	I, II, III, IV, V, VI	PWM	• Output is bidirectional and the converter is simple in design • It can operate with high effective duty cycles • It is suitable for low-power small satellites applications where there is no need of galvanic isolation and reduced complexity, volume, and cost are prioritized over reliability. • It requires auxiliary start up circuit
[94]	Z-source	120	I, II, III, IV	DCC	• Output is unidirectional and the converter operates with low duty cycle and high efficiency • It can boost voltage in different operation modes with acceptable voltage gain. • Voltage stress on power switches is low.

TABLE 5. *(Continued.)* **Comparison of Control/Hardware Limitations and Key Features for the TPC Topologies.**

[95]	Sepic voltage doubler	200	II, III, IV, V	DCC	• Output is unidirectional • It is suitable for high step-up voltage applications
[65]	Half bridge with synchronous rectification	120	I, II, III, IV, V	PWM	• Output port is unidirectional • It is suitable for standalone renewable power systems • It is derived from integrated half bridge converter topology, a forward–flyback converter and a bidirectional switching cell as a buck converter • The converter with post-regulation features the ZVS of all the switches while with synchronous regulation it features the minimum number of devices
[68]	Two interleaved buck/boost converter and a secondary side full-bridge converter	600	I, II, III, IV, V	PWM and PS	• Output is unidirectional and bidirectional flow can be achieved by using four quadrant switches • Decoupled control among three ports is achievable • It is possible to extend the ZVS range of the switches • Improved efficiency • Low voltage/current ripple on the PV port by means of interleaving the two bidirectional buck/boost converters
[70]	Two interleaved buck/boost converter and a secondary side bridgeless boost rectifier	500	I, II, III, IV, V	PWM plus PS	• Output is unidirectional and bidirectional flow can be achieved by using four quadrant switches • Low voltage/current ripple on the PV port by means of interleaving the two bidirectional buck/boost converters • Tight port voltage restrictions exist on the input ports
[29]	Full bridge buck/boost and a bridge rectifier	300	I, II, III, IV, V	PWM	• Output is unidirectional
[73]	Interleaved-boost full-bridge converter and DAB	1000	I, II, III, IV, V, VI	PWM and DCC	• Improved transformer utilization • Interleaved boost full bridge PWM is similar to two interleaved buck boost converter • It has automatic current balancing capability • It provides flexible power exchange among ports
[23]	Interleaved boost full bridge converter and bridge rectifier	1000	I, II, III, IV, V	PWM	• Output is unidirectional
[14]	Interleaved half bridge converters and bridge rectifier	500	I, II, III, IV, V	PWM	• Output is unidirectional • The circulating current is eliminated • Port voltage restrictions are minimized by extending the voltage gain of the load port • Filter circuit becomes simple and small • It is possible to achieve ZVS for all primary side switches
[69]	Interleaved boost converter and LLC resonant converter	500	I, II, III, IV, V	PWM and PFM Hybrid Modulated	• Output is unidirectional • Low input current ripple that is needed for PV port • With the help of interleaved boost converter and resonant tank, it is possible to achieve ZVS for all primary switches and ZCS for all secondary rectifier diodes over full operating range • It reduces switching loses and electromagnetic interference • The output port has to be tightly regulated to meet load requirements
[74]	LCL resonant converter	120	I, II, III, IV, V	PFM	• Output is unidirectional • It features minimum number of switches than [23] [14] [69]
[77]	DAB derived converter	1500	I, II, III, IV, V, VI	DCC	• Output is fully bidirectional, and ports are symmetrical • Port voltage restrictions are eliminated. • Decoupled power flow is possible for fast dynamic response
[86]	DAB derived converter	1000	I, II, III, IV, V, VI	PS	• Output is bidirectional, and ports are symmetrical • The HF transformer winding configuration enables variable turns ratio • It allows a wider input/output range
[26]	DAB derived series resonant converter	500	I, II, III, IV, V, VI	PS	• Output is bidirectional, and ports are symmetrical. • Reduced switching losses due to soft switching operation
[105]	DAB derived converter	50,000	I, II, III, IV, V, VI	DCC plus PS	• Output is bidirectional and this provides modular multilevel structure for low and medium voltage applications. • The power flow control follows a simple mathematical rule that significantly reduces computational burden • Circulating current is inherently prevented • It requires very simple transformer design approach
[106]	DAB derived converter	150,000	I, II, III, IV, V, VI	PS	• Output is bidirectional and SiC-based H-bridge converter is used to derive the TPC • High efficiency is achieved with SiC switching technologies
[107], [108], [109]	DAB derived converter	800	I, II, III, IV, V, VI	DCC plus PS	• Output is bidirectional and it reduces switching losses • Reduced noise peaks and improved EMI performance

TABLE 5. *(Continued.)* **Comparison of Control/Hardware Limitations and Key Features for the TPC Topologies.**

[110]	DAB derived series resonant converter	2000	I, II, III, IV, V, VI	DCC plus PS	• Output is bidirectional and it reduces RMS tank current • It can achieve ZVS for all switches across the entire AC line cycle and maintain higher efficiency at all operating points • It can modulate the input currents and can provide power factor correction to maintain power quality at the grid side • The results validate the converter ability to modulate the input currents required for PFC action and also achieve zero voltage switching across the entire AC line cycle.
[111]	Isolated resonant converter	500	I, II, III, IV, V	PS	• Output is unidirectional; however, it can be made bidirectional with bidirectional switches.
[112]	DAB derived series resonant converter	6600	I, II, III, IV, V, VI	PFM	• Output is bidirectional
[113]	DAB derived converter	300	I, II, III, IV, V, VI	PWM	• Output is bidirectional and ports are symmetrical • Auxiliary switches are required to guarantee zero circulating current flow between different ports

TABLE 6. **Recommendation for the Choice of TPC Topologies Based on Requirements and applications.**

System requirements/applications	Preferred topologies with characteristics
Standalone power systems applications	Power flow is unidirectional and therefore, it is not mandatory for TPC to have bidirectional power flow capability between BES and load.
Grid-connected power systems applications	Power flow could be bidirectional and hence it is an essential design requirement for TPC to allow bidirectional power flow between BES and load
Low power applications	Non-isolated topologies are preferred where there are no isolation requirements between the ports
Medium and high-power applications	Partly isolated and isolated topologies are preferred where there are isolation requirements between the ports
TPC topologies with direct AC port	Boost derived and Z-source inverters are preferred for low power applications where there are no isolation requirements

isolated topologies. The key parameters of these topologies such as power ratings, port voltages, switching frequencies, component counts and values, average efficiencies are shown in Tables 1-3 respectively. These TPC topologies are further classified based on their topological configurations as presented in Table 5. The detailed comparison of key features and limitations, control complexities and important advantages and disadvantages of the individual TPC arrangements are discussed and presented in Table 5. It is evident from Tables 1-4 that the choice of the TPC topologies depends on systems requirements and applications. For example, it is not an essential design requirement for TPC topologies to have bidirectional power flow capabilities between BES and load if the TPC topologies are intended for use in standalone power systems employing PV and BES. In an application where there are no isolation requirements between the load and BES terminal, the non-isolated topologies might be an appropriate choice. From the comparative study and above discussion, it can be established that non-isolated topologies are highly efficient and cost effective and are well suited for low power applications where there is no isolation needed, whereas isolated topologies are well suited for medium and high power applications where isolation requirements are necessary. Among two different isolated TPC arrangements, the fully isolated TPC based on the DAB/TAB derived configuration seems to be a suitable topology and can be reconfigured to use in grid-interactive PV-BES integrated systems. The review also explored converter topologies with a direct AC port in Section V. It identified different topologies such as the boost derived converter, Z-source inverter, matrix converter and DAB with back-to-back converter. The boost derived topology and Z-source inverter might be suitable for low power applications, however, these topologies cannot be used where an isolation requirement exists. Considering these factors, DAB derived topologies seem to be an appropriate topology. This review also examines and discusses the options to reconfigure a DAB/TAB for full four quadrant ac output port operations for grid interactive systems. The study found that the direct full four quadrant ac output port for the grid integrated PV-BES system is implemented by either a direct form matrix converter approach or DAB and a back-to-back converter with a small dc-link capacitor. However, there are some complexities in the modulation and commutation process of a matrix converter. Therefore, the future research must address the challenges in modular, cost-effective, and highly efficient converter design. The future research should also address the challenges to develop innovative control strategies for converters to minimize the losses and improve the power density. For isolated topologies, the research challenge is to meet compact converter design requirements with technological innovation in HF transformer designs, lower component counts, and fast semiconductor switches to meet the lower cost and higher efficiency targets. Table 6 provides the best recommendations for the choice of TPC topologies based on system requirements and applications.

VIII. CONCLUSION

The use of PV and BES systems is gradually increasing in residential applications. The effective utilization of the PV and BES systems requires enabling power converter technologies. TPCs are an alternative means to implement single stage power electronics conversion to support PV and BES system utilization and integrations, having fundamental features such as the MPPT option for PV and charging/discharging capabilities for battery port. In this paper, a comprehensive review is carried out on a variety of dc-dc TPC topologies that are reported in recent publications. This paper provides a framework that systematically explores the full range of technical benefits and limitations of each TPC topology. This extensive review with its thorough discussion provides a useful framework and a strong foundation for researchers working on future TPC topology developments.

REFERENCES

[1] T. Ackermann, G. Andersson, and L. Söder, "Distributed generation: A definition," *Electr. Power Syst. Res.*, vol. 57, no. 3, pp. 195–204, Apr. 2001.

[2] Q. Li and P. Wolfs, "A review of the single phase photovoltaic module integrated converter topologies with three different DC link configurations," *IEEE Trans. Power Electron.*, vol. 23, no. 3, pp. 1320–1333, May 2008.

[3] C. N. Truong, "Maximizing solar home battery systems' contribution to the energy transition of the power system," in *Proc. Conf. Sustain. Energy Supply Energy Storage Syst.*, 2017, pp. 1–8.

[4] *Global Market Outlook for Solar Power 2022–2026*. Accessed: Sep. 17, 2022. [Online]. Available: https://www.solarpowereurope.org/

[5] (Sep. 17, 2022). *Global Market Outlook for Photovoltaics 2014–2018*. [Online]. Available: http://www.epia.org/news/publications/

[6] M. M. Haque and P. Wolfs, "A review of high PV penetrations in LV distribution networks: Present status, impacts and mitigation measures," *Renew. Sustain. Energy Rev.*, vol. 62, pp. 1195–1208, Sep. 2016.

[7] (Sep. 17, 2022). *Tracking Energy Integration 2021*. [Online]. Available: https://www.iea.org/reports/tracking-energy-integration-2021

[8] A. K. Bhattacharjee, N. Kutkut, and I. Batarseh, "Review of multiport converters for solar and energy storage integration," *IEEE Trans. Power Electron.*, vol. 34, no. 2, pp. 1431–1445, Feb. 2019.

[9] (Jun. 25, 2019). *Little Box Challenge by CE+T Power*. [Online]. Available: http://littleboxchallengecetpower.com/

[10] H. Wu, P. Xu, H. Hu, Z. Zhou, and Y. Xing, "Multiport converters based on integration of full-bridge and bidirectional DC–DC topologies for renewable generation systems," *IEEE Trans. Ind. Electron.*, vol. 61, no. 2, pp. 856–869, Feb. 2014.

[11] W. Hu, H. Wu, Y. Xing, and K. Sun, "A full-bridge three-port converter for renewable energy application," in *Proc. IEEE Appl. Power Electron. Conf. Expo. (APEC)*, Mar. 2014, pp. 57–62.

[12] H. Tao, A. Kotsopoulos, J. L. Duarte, and M. A. M. Hendrix, "Family of multiport bidirectional DC-DC converters," *IEE Proc.-Electr. Power Appl.*, vol. 153, no. 3, pp. 451–458, May 2006.

[13] M. M. Haque, P. Wolfs, and S. Alahakoon, "Small signal modeling and control of isolated three port DC-DC converter for PV-battery system," in *Proc. IEEE Region Humanitarian Technol. Conf. (R-HTC)*, Dec. 2017, pp. 263–266.

[14] H. Wu, K. Sun, L. Zhu, and Y. Xing, "An interleaved half-bridge three-port converter with enhanced power transfer capability using three-leg rectifier for renewable energy applications," *IEEE J. Emerg. Sel. Topics Power Electron.*, vol. 4, no. 2, pp. 606–616, Jun. 2016.

[15] P. Zhang, Y. Chen, and Y. Kang, "Nonisolated wide operation range three-port converters with variable structures," *IEEE J. Emerg. Sel. Topics Power Electron.*, vol. 5, no. 2, pp. 854–869, Sep. 2017.

[16] *Powerwall | The Tesla Home Battery*. Accessed: Feb. 22, 2017. [Online]. Available: https://www.tesla.com/en_AU/powerwall

[17] W. Jiang and B. Fahimi, "Multi-port power electric interface for renewable energy sources," in *Proc. 24th Annu. IEEE Appl. Power Electron. Conf. Expo.*, Feb. 2009, pp. 347–352.

[18] H. Tao, J. L. Duarte, and M. A. M. Hendrix, "Multiport converters for hybrid power sources," in *Proc. IEEE Power Electron. Spec. Conf.*, Jun. 2008, pp. 3412–3418.

[19] N. Zhang, D. Sutanto, and K. M. Muttaqi, "A review of topologies of three-port DC–DC converters for the integration of renewable energy and energy storage system," *Renew. Sustain. Energy Rev.*, vol. 56, pp. 388–401, Apr. 2016.

[20] S. Khosrogorji, M. Ahmadian, H. Torkaman, and S. Soori, "Multi-input DC/DC converters in connection with distributed generation units—A review," *Renew. Sustain. Energy Rev.*, vol. 66, pp. 360–379, Dec. 2016.

[21] J. Garcia, R. Georgious, P. Garcia, and A. Navarro-Rodriguez, "Non-isolated high-gain three-port converter for hybrid storage systems," in *Proc. IEEE Energy Convers. Congr. Expo. (ECCE)*, Sep. 2016, pp. 1–8.

[22] H. Wu, Y. Xing, Y. Xia, and K. Sun, "A family of non-isolated three-port converters for stand-alone renewable power system," in *Proc. IECON 37th Annu. Conf. IEEE Ind. Electron. Soc.*, Nov. 2011, pp. 1030–1035.

[23] M. C. Mira, Z. Zhang, A. Knott, and M. A. E. Andersen, "Analysis, design, modeling, and control of an interleaved-boost full-bridge three-port converter for hybrid renewable energy systems," *IEEE Trans. Power Electron.*, vol. 32, no. 2, pp. 1138–1155, Feb. 2017.

[24] Y.-K. Tran and D. Dujic, "A multiport isolated DC-DC converter," in *Proc. IEEE Appl. Power Electron. Conf. Expo. (APEC)*, Mar. 2016, pp. 156–162.

[25] H. Tao, A. Kotsopoulos, J. L. Duarte, and M. A. M. Hendrix, "Transformer-coupled multiport ZVS bidirectional DC–DC converter with wide input range," *IEEE Trans. Power Electron.*, vol. 23, no. 2, pp. 771–781, Mar. 2008.

[26] H. Krishnaswami and N. Mohan, "Three-port series-resonant DC–DC converter to interface renewable energy sources with bidirectional load and energy storage ports," *IEEE Trans. Power Electron.*, vol. 24, no. 10, pp. 2289–2297, Oct. 2009.

[27] M. R. Al-Soeidat, H. Aljarajreh, H. A. Khawaldeh, D. D. Lu, and J. Zhu, "A reconfigurable three-port DC–DC converter for integrated PV-battery system," *IEEE J. Emerg. Sel. Topics Power Electron.*, vol. 8, no. 4, pp. 3423–3433, Dec. 2020.

[28] H. Wu, Y. Jia, F. Yang, L. Zhu, and Y. Xing, "Two-stage isolated bidirectional DC–AC converters with three-port converters and two DC buses," *IEEE J. Emerg. Sel. Topics Power Electron.*, vol. 8, no. 4, pp. 4428–4439, Dec. 2020.

[29] H. Wu, K. Sun, R. Chen, H. Hu, and Y. Xing, "Full-bridge three-port converters with wide input voltage range for renewable power systems," *IEEE Trans. Power Electron.*, vol. 27, no. 9, pp. 3965–3974, Sep. 2012.

[30] M. M. Haque, P. Wolfs, and S. Alahakoon, "Dual active bridge and matrix converter based three-port converter topology for grid interactive PV-battery system," in *Proc. Australas. Universities Power Eng. Conf. (AUPEC)*, Nov. 2017, pp. 1–6.

[31] M. M. Haque, P. Wolfs, and S. Alahakoon, "Three-port converter with decoupled power control strategies for residential PV-battery system," in *Proc. IEEE Int. Conf. Ind. Electron. Sustain. Energy Syst. (IESES)*, Jan. 2018, pp. 180–185.

[32] M. M. Haque, P. Wolfs, and S. Alahakoon, "Small signal modeling and control of isolated three port DC-DC converter for PV-battery system," in *Proc. IEEE Region Humanitarian Technol. Conf. (R-HTC)*, Dec. 2017, pp. 263–266.

[33] P. Zhang, Y. Chen, and Y. Kang, "Nonisolated wide operation range three-port converters with variable structures," *IEEE J. Emerg. Sel. Topics Power Electron.*, vol. 5, no. 2, pp. 854–869, Jun. 2017.

[34] P. Zhang, Y. Chen, Z. Lu, and Y. Kang, "The cost-efficient, common-ground, non-isolated three-port converter deduced from the single-inductor dual-output (SIDO) topology," in *Proc. IEEE Appl. Power Electron. Conf. Expo. (APEC)*, Mar. 2015, pp. 2020–2025.

[35] H. Zhu, D. Zhang, B. Zhang, and Z. Zhou, "A nonisolated three-port DC–DC converter and three-domain control method for PV-battery power systems," *IEEE Trans. Ind. Electron.*, vol. 62, no. 8, pp. 4937–4947, Aug. 2015.

[36] L.-J. Chien, C.-C. Chen, J.-F. Chen, and Y.-P. Hsieh, "Novel three-port converter with high-voltage gain," *IEEE Trans. Power Electron.*, vol. 29, no. 9, pp. 4693–4703, Sep. 2014.

[37] H. Wu, K. Sun, S. Ding, and Y. Xing, "Topology derivation of nonisolated three-port DC-DC converters from DIC and DOC," *IEEE Trans. Power Electron.*, vol. 28, no. 7, pp. 3297–3307, Jul. 2013.

[38] Y. Chen, A. Q. Huang, and X. Yu, "A high step-up three-port DC-DC converter for stand-alone PV/battery power systems," *IEEE Trans. Power Electron.*, vol. 28, no. 11, pp. 5049–5062, Nov. 2013.
[39] K. Tomas-Manez, A. Anthon, Z. Zhang, Z. Ouyang, and T. Franke, "High efficiency non-isolated three port DC-DC converter for PV-battery systems," in *Proc. IEEE 8th Int. Power Electron. Motion Control Conf. (IPEMC-ECCE Asia)*, May 2016, pp. 1806–1812.
[40] M. Zhang, Y. Xing, H. Wu, Y. Lu, and K. Sun, "Performance evaluation of a non-isolated bidirectional three-port power converter for energy storage applications," in *Proc. IEEE 8th Int. Power Electron. Motion Control Conf. (IPEMC-ECCE Asia)*, May 2016, pp. 2703–2708.
[41] M. C. Mira, A. Knott, and M. A. E. Andersen, "A three-port topology comparison for a low power stand-alone photovoltaic system," in *Proc. Int. Power Electron. Conf. (IPEC-Hiroshima ECCE ASIA)*, May 2014, pp. 506–513.
[42] Y. Chen, G. Wen, L. Peng, Y. Kang, and J. Chen, "A family of cost-efficient non-isaolated single-inductor three-port converters for low power stand-alone renewable power applications," in *Proc. 28th Annu. IEEE Appl. Power Electron. Conf. Expo. (APEC)*, Mar. 2013, pp. 1083–1088.
[43] Y. M. Chen, X. Yu, and A. Q. Huang, "A new nonisolated three-port DC-DC converter with high step-up/down ratio," in *Proc. IEEE Energy Convers. Congr. Expo.*, Sep. 2012, pp. 1520–1526.
[44] Y. Chen, P. Zhang, X. Zou, and Y. Kang, "Dynamical modeling of the non-isolated single-inductor three-port converter," in *Proc. IEEE Appl. Power Electron. Conf. Expo. (APEC)*, Mar. 2014, pp. 2067–2073.
[45] A. Khaligh, J. Cao, and Y.-J. Lee, "A multiple-input DC-DC converter topology," *IEEE Trans. Power Electron.*, vol. 24, no. 3, pp. 862–868, Mar. 2009.
[46] K. Gummi and M. Ferdowsi, "Double-input DC–DC power electronic converters for electric-drive Vehicles—Topology exploration and synthesis using a single-pole triple-throw switch," *IEEE Trans. Ind. Electron.*, vol. 57, no. 2, pp. 617–623, Feb. 2010.
[47] A. Nahavandi, M. T. Hagh, M. B. B. Sharifian, and S. Danyali, "A non-isolated multiinput multioutput DC-DC boost converter for electric vehicle applications," *IEEE Trans. Power Electron.*, vol. 30, no. 4, pp. 1818–1835, Apr. 2015.
[48] A. I, S. Senthilkumar, D. Biswas, and M. Kaliamoorthy, "Dynamic power management system employing a single-stage power converter for standalone solar PV applications," *IEEE Trans. Power Electron.*, vol. 33, no. 12, pp. 10352–10362, Dec. 2018.
[49] A. Hintz, U. R. Prasanna, and K. Rajashekara, "Novel modular multiple-input bidirectional DC–DC power converter (MIPC) for HEV/FCV application," *IEEE Trans. Ind. Electron.*, vol. 62, no. 5, pp. 3163–3172, May 2015.
[50] H. Wu, J. Zhang, and Y. Xing, "A family of multiport buck–boost converters based on DC-link-inductors (DLIs)," *IEEE Trans. Power Electron.*, vol. 30, no. 2, pp. 735–746, Feb. 2015.
[51] M. Marchesoni and C. Vacca, "New DC–DC converter for energy storage system interfacing in fuel cell hybrid electric vehicles," *IEEE Trans. Power Electron.*, vol. 22, no. 1, pp. 301–308, Jan. 2007.
[52] G. Chen, Y. Deng, J. Dong, Y. Hu, L. Jiang, and X. He, "Integrated multiple-output synchronous buck converter for electric vehicle power supply," *IEEE Trans. Veh. Technol.*, vol. 66, no. 7, pp. 5752–5761, Jul. 2017.
[53] E. C. dos Santos, "Dual-output dc-dc buck converters with bidirectional and unidirectional characteristics," *IET Power Electron.*, vol. 6, no. 5, pp. 999–1009, May 2013.
[54] N. Katayama, S. Tosaka, T. Yamanaka, M. Hayase, K. Dowaki, and S. Kogoshi, "New topology for DC–DC converters used in fuel cell–electric double layer capacitor hybrid power source systems for mobile devices," *IEEE Trans. Ind. Appl.*, vol. 52, no. 1, pp. 313–321, Jan. 2016.
[55] O. Ray, A. P. Josyula, S. Mishra, and A. Joshi, "Integrated dual-output converter," *IEEE Trans. Ind. Electron.*, vol. 62, no. 1, pp. 371–382, Jan. 2015.
[56] Y. Chen, P. Zhang, X. Zou, and Y. Kang, "Dynamical modeling of the non-isolated single-inductor three-port converter," in *Proc. IEEE Appl. Power Electron. Conf. Expo. (APEC)*, Mar. 2014, pp. 2067–2073.
[57] Y. Chen, G. Wen, L. Peng, Y. Kang, and J. Chen, "A family of cost-efficient non-isaolated single-inductor three-port converters for low power stand-alone renewable power applications," in *Proc. 28th Annu. IEEE Appl. Power Electron. Conf. Expo. (APEC)*, Mar. 2013, pp. 1083–1088.
[58] J. D. Dasika, B. Bahrani, M. Saeedifard, A. Karimi, and A. Rufer, "Multivariable control of single-inductor dual-output buck converters," *IEEE Trans. Power Electron.*, vol. 29, no. 4, pp. 2061–2070, Apr. 2014.
[59] C.-S. Huang, D. Chen, C.-J. Chen, and K. H. Liu, "Mix-voltage conversion for single-inductor dual-output buck converters," *IEEE Trans. Power Electron.*, vol. 25, no. 8, pp. 2106–2114, Aug. 2010.
[60] Y.-C. Liu and Y.-M. Chen, "A systematic approach to synthesizing multi-input DC–DC converters," *IEEE Trans. Power Electron.*, vol. 24, no. 1, pp. 116–127, Jan. 2009.
[61] Y. Li, X. Ruan, D. Yang, F. Liu, and C. K. Tse, "Synthesis of multiple-input DC/DC converters," *IEEE Trans. Power Electron.*, vol. 25, no. 9, pp. 2372–2385, Sep. 2010.
[62] H. Wu, Y. Xing, Y. Xia, and K. Sun, "A family of non-isolated three-port converters for stand-alone renewable power system," in *Proc. IECON 37th Annu. Conf. IEEE Ind. Electron. Soc.*, Nov. 2011, pp. 1030–1035.
[63] P. Zhang, Y. Chen, Z. Lu, and Y. Kang, "The cost-efficient, common-ground, non-isolated three-port converter deduced from the single-inductor dual-output (SIDO) topology," in *Proc. IEEE Appl. Power Electron. Conf. Expo. (APEC)*, Mar. 2015, pp. 2020–2025.
[64] Z. Qian, O. Abdel-Rahman, H. Al-Atrash, and I. Batarseh, "Modeling and control of three-port DC/DC converter interface for satellite applications," *IEEE Trans. Power Electron.*, vol. 25, no. 3, pp. 637–649, Mar. 2010.
[65] H. Wu, R. Chen, J. Zhang, Y. Xing, H. Hu, and H. Ge, "A family of three-port half-bridge converters for a stand-alone renewable power system," *IEEE Trans. Power Electron.*, vol. 26, no. 9, pp. 2697–2706, Sep. 2011.
[66] Z. Wang and H. Li, "An integrated three-port bidirectional DC–DC converter for PV application on a DC distribution system," *IEEE Trans. Power Electron.*, vol. 28, no. 10, pp. 4612–4624, Oct. 2013.
[67] J. Zeng, W. Qiao, and L. Qu, "Modeling and control of a three-port DC-DC converter for PV-battery systems," in *Proc. IEEE Appl. Power Electron. Conf. Expo.*, Mar. 2015, pp. 1768–1773.
[68] J. Zhang, H. Wu, X. Qin, and Y. Xing, "PWM plus secondary-side phase-shift controlled soft-switching full-bridge three-port converter for renewable power systems," *IEEE Trans. Ind. Electron.*, vol. 62, no. 11, pp. 7061–7072, Nov. 2015.
[69] X. Sun, Y. Shen, W. Li, and H. Wu, "A PWM and PFM hybrid modulated three-port converter for a standalone PV/battery power system," *IEEE J. Emerg. Sel. Topics Power Electron.*, vol. 3, no. 4, pp. 984–1000, Dec. 2015.
[70] H. Wu, J. Zhang, X. Qin, T. Mu, and Y. Xing, "Secondary-side-regulated soft-switching full-bridge three-port converter based on bridgeless boost rectifier and bidirectional converter for multiple energy interface," *IEEE Trans. Power Electron.*, vol. 31, no. 7, pp. 4847–4860, Jul. 2016.
[71] X. Sun, Y. Shen, and W. Li, "A novel LLC integrated three-port DC-DC converter for stand-alone PV/battery system," in *Proc. IEEE Conf. Expo. Transp. Electrific. Asia–Pacific (ITEC Asia–Pacific)*, Aug. 2014, pp. 1–6.
[72] H. Al-Atrash, M. Pepper, and I. Batarseh, "A zero-voltage switching three-port isolated full-bridge converter," in *Proc. INTELEC 28th Int. Telecommun. Energy Conf.*, Sep. 2006, pp. 1–8.
[73] M. Uno, M. Sato, Y. Tada, S. Iyasu, N. Kobayashi, and Y. Hayashi, "Partially-isolated multiport converter with automatic current balancing interleaved PWM converter and improved transformer utilization for EV batteries," *IEEE Trans. Transport. Electrific.*, early access, May 13, 2022, doi: 10.1109/TTE.2022.3175032.
[74] J. Zeng, W. Qiao, and L. Qu, "An isolated three-port bidirectional DC-DC converter for photovoltaic systems with energy storage," *IEEE Trans. Ind. Appl.*, vol. 51, no. 4, pp. 3493–3503, Jul./Aug. 2015.
[75] T. Qian, K. Guo, and C. Qian, "A combined three-port LLC structure for adaptive power flow adjustment of PV systems," *IEEE Trans. Power Electron.*, vol. 35, no. 10, pp. 10413–10422, Oct. 2020.
[76] J. Zeng, W. Qiao, and L. Qu, "A LCL-resonant isolated multiport DC-DC converter for power management of multiple renewable energy sources," in *Proc. IEEE Energy Convers. Congr. Expo.*, Sep. 2013, pp. 2347–2354.
[77] C. Zhao, S. D. Round, and J. W. Kolar, "An isolated three-port bidirectional DC-DC converter with decoupled power flow management," *IEEE Trans. Power Electron.*, vol. 23, no. 5, pp. 2443–2453, Sep. 2008.
[78] H. Krishnaswami and N. Mohan, "Constant switching frequency series resonant three-port bi-directional DC-DC converter," in *Proc. IEEE Power Electron. Spec. Conf.*, Jun. 2008, pp. 1640–1645.
[79] S. Y. Kim, I. Jeong, K. Nam, and H.-S. Song, "Three-port full bridge converter application as a combined charger for PHEVs," in *Proc. IEEE Vehicle Power Propuls. Conf.*, Sep. 2009, pp. 461–465.

[80] F. Jauch and J. Biela, "Single-phase single-stage bidirectional isolated ZVS AC-DC converter with PFC," in *Proc. 15th Int. Power Electron. Motion Control Conf. (EPE/PEMC)*, Sep. 2012, pp. 1–9.

[81] S. Baek, S. Roy, S. Bhattacharya, and S. Kim, "Power flow analysis for 3-port 3-phase dual active bridge DC/DC converter and design validation using high frequency planar transformer," in *Proc. IEEE Energy Convers. Congr. Expo.*, Sep. 2013, pp. 388–395.

[82] B. Zhao, S. Qiang, W. Liu, and Y. Sun, "Overview of dual-active-bridge isolated bidirectional DC-DC converter for high-frequency-link power-conversion system," *IEEE Trans. Power Electron.*, vol. 29, no. 8, pp. 4091–4106, Aug. 2014.

[83] H. Zhu, D. Zhang, H. S. Athab, B. Wu, and Y. Gu, "PV isolated three-port converter and energy-balancing control method for PV-battery power supply applications," *IEEE Trans. Ind. Electron.*, vol. 62, no. 6, pp. 3595–3606, Jun. 2015.

[84] A. Ajami and P. Asadi Shayan, "Soft switching method for multiport DC/DC converters applicable in grid connected clean energy sources," *IET Power Electron.*, vol. 8, no. 7, pp. 1246–1254, Jul. 2015.

[85] R. Chattopadhyay and S. Bhattacharya, "Power flow control and ZVS analysis of three limb high frequency transformer based three-port DAB," in *Proc. IEEE Appl. Power Electron. Conf. Expo. (APEC)*, Mar. 2016, pp. 778–785.

[86] Z. Ouyang and M. A. E. Andersen, "Integrated three-port DC-DC converter for photovoltaic (PV) battery stand-alone systems," in *Proc. Int. Exhib. Conf. Power Electron., Intell. Motion, Renew. Energy Energy Manage.*, 2016, pp. 1–8.

[87] Y. Hu, W. Xiao, W. Cao, B. Ji, and D. J. Morrow, "Three-port DC-DC converter for stand-alone photovoltaic systems," *IEEE Trans. Power Electron.*, vol. 30, no. 6, pp. 3068–3076, Jun. 2015.

[88] R. W. A. A. De Doncker, D. M. Divan, and M. H. Kheraluwala, "A three-phase soft-switched high-power-density DC/DC converter for high-power applications," *IEEE Trans. Ind. Appl.*, vol. 27, no. 1, pp. 63–73, Feb. 1991.

[89] R. P. Severns and G. Bloom, *Modern Dc-to-Dc Switchmode Power Converter Circuits*. New York, NY, USA: Van Nostrand Reinhold, 1985.

[90] M. M. Haque, P. Wolfs, and S. Alahakoon, "Dual active bridge and matrix converter based three-port converter topology for grid interactive PV-battery system," in *Proc. 27th Australas. Universities Power Eng. Conf.*, Melbourne, VIC, Australia, Nov. 2017, pp. 1–6.

[91] H. Nagata and M. Uno, "Nonisolated PWM three-port converter realizing reduced circuit volume for satellite electrical power systems," *IEEE Trans. Aerosp. Electron. Syst.*, vol. 56, no. 5, pp. 3394–3408, Oct. 2020.

[92] L. Senapati, A. K. Panda, M. M. Garg, and R. K. Lenka, "A systematic approach to synthesize a non-isolated TPCC with fully reconfigurable structure for RES," *IEEE Trans. Circuits Syst. II, Exp. Briefs*, vol. 69, no. 7, pp. 3314–3318, Jul. 2022.

[93] M. R. Al-Soeidat, H. Aljarajreh, H. A. Khawaldeh, D. D. Lu, and J. Zhu, "A reconfigurable three-port DC–DC converter for integrated PV-battery system," *IEEE J. Emerg. Sel. Topics Power Electron.*, vol. 8, no. 4, pp. 3423–3433, Dec. 2020.

[94] S. Rostami, V. Abbasi, and M. Parastesh, "Design and implementation of a multiport converter using Z-source converter," *IEEE Trans. Ind. Electron.*, vol. 68, no. 10, pp. 9731–9741, Oct. 2021.

[95] R. Cheraghi, E. Adib, and M. S. Golsorkhi, "A nonisolated high step-up three-port soft-switched converter with minimum switches," *IEEE Trans. Ind. Electron.*, vol. 68, no. 10, pp. 9358–9365, Oct. 2021.

[96] R. Faraji, L. Ding, M. Esteki, N. Mazloum, and S. A. Khajehoddin, "Soft-switched single inductor single stage multiport bidirectional power converter for hybrid energy systems," *IEEE Trans. Power Electron.*, vol. 36, no. 10, pp. 11298–11315, Oct. 2021.

[97] H. Aljarajreh, D. D.-C. Lu, Y. P. Siwakoti, and C. K. Tse, "A nonisolated three-port DC–DC converter with two bidirectional ports and fewer components," *IEEE Trans. Power Electron.*, vol. 37, no. 7, pp. 8207–8216, Jul. 2022.

[98] T.-J. Liang, K.-F. Liao, K.-H. Chen, and S.-M. Chen, "Three-port converter with single coupled inductor for high step-up applications," *IEEE Trans. Power Electron.*, vol. 37, no. 8, pp. 9840–9849, Aug. 2022.

[99] H. Al-Atrash and I. Batarseh, "Boost-integrated phase-shift full-bridge converter for three-port interface," in *Proc. IEEE Power Electron. Spec. Conf.*, Jun. 2007, pp. 2313–2321.

[100] W. Li, J. Xiao, Y. Zhao, and X. He, "PWM plus phase angle shift (PPAS) control scheme for combined multiport DC/DC converters," *IEEE Trans. Power Electron.*, vol. 27, no. 3, pp. 1479–1489, Mar. 2012.

[101] C. Zhao and J. W. Kolar, "A novel three-phase three-port UPS employing a single high-frequency isolation transformer," in *Proc. IEEE 35th Annu. Power Electron. Spec. Conf.*, Jun. 2004, pp. 4135–4141.

[102] J. L. Duarte, M. Hendrix, and M. G. Simoes, "Three-port bidirectional converter for hybrid fuel cell systems," *IEEE Trans. Power Electron.*, vol. 22, no. 2, pp. 480–487, Mar. 2007.

[103] M. N. Kheraluwala, R. W. Gascoigne, D. M. Divan, and E. D. Baumann, "Performance characterization of a high-power dual active bridge DC-to-DC converter," *IEEE Trans. Ind. Appl.*, vol. 28, no. 6, pp. 1294–1301, Dec. 1992.

[104] R. W. D. Doncker, D. M. Divan, and M. H. Kheraluwala, "A three-phase soft-switched high power density DC/DC converter for high power applications," in *Proc. Conf. Rec. IEEE Ind. Appl. Soc. Annu. Meeting*, Jan. 1988, pp. 796–805.

[105] S. Zhao, Y. Chen, S. Cui, B. J. Mortimer, and R. W. De Doncker, "Three-port bidirectional operation scheme of modular-multilevel DC–DC converters interconnecting MVDC and LVDC grids," *IEEE Trans. Power Electron.*, vol. 36, no. 7, pp. 7342–7348, Jul. 2021.

[106] Y. Wu, M. H. Mahmud, S. Christian, R. A. Fantino, R. A. Gomez, Y. Zhao, and J. C. Balda, "A 150-kW 99% efficient all-silicon-carbide triple-active-bridge converter for solar-plus-storage systems," *IEEE J. Emerg. Sel. Topics Power Electron.*, vol. 10, no. 4, pp. 3496–3510, Aug. 2022.

[107] S. Dey and A. Mallik, "Multivariable-modulation-based conduction loss minimization in a triple-active-bridge converter," *IEEE Trans. Power Electron.*, vol. 37, no. 6, pp. 6599–6612, Jun. 2022.

[108] S. Dey, A. Mallik, and A. Akturk, "Multi-variable multi-constraint optimization of triple active bridge DC-DC converter with conduction loss minimization," in *Proc. IEEE Appl. Power Electron. Conf. Expo. (APEC)*, Mar. 2022, pp. 355–360.

[109] S. Dey, A. Mallik, and A. Akturk, "Investigation of ZVS criteria and optimization of switching loss in a triple active bridge converter using penta-phase-shift modulation," *IEEE J. Emerg. Sel. Topics Power Electron.*, vol. 10, no. 6, pp. 7014–7028, Dec. 2022.

[110] D. B. Yelaverthi, M. Mansour, H. Wang, and R. Zane, "Triple active bridge series resonant converter for three-phase unfolding based isolated converters," in *Proc. IECON 45th Annu. Conf. IEEE Ind. Electron. Soc.*, Oct. 2019, pp. 4924–4930.

[111] E. Asa, K. Colak, D. Czarkowski, and B. Ozpineci, "Analysis of high frequency AC link isolated three port resonant converter for UAV applications," in *Proc. IEEE Appl. Power Electron. Conf. Expo. (APEC)*, Mar. 2020, pp. 1679–1684.

[112] M. Kumar, P. M. Barbosa, J. M. Ruiz, J. Minli, and S. Hao, "Isolated three-port bidirectional DC-DC converter for electric vehicle applications," in *Proc. IEEE Appl. Power Electron. Conf. Expo. (APEC)*, Mar. 2022, pp. 2000–2007.

[113] M. I. Marei, B. N. Alajmi, I. Abdelsalam, and N. A. Ahmed, "An integrated topology of three-port DC-DC converter for PV-battery power systems," *IEEE Open J. Ind. Electron. Soc.*, vol. 3, pp. 409–419, 2022.

[114] F. Wu, W. Liu, K. Wang, and G. Wang, "Modeling and closed-loop control of three-port isolated current-fed resonant DC-DC converter," *IEEE Trans. Transport. Electrific.*, early access, Aug. 11, 2022, doi: 10.1109/TTE.2022.3198288.

[115] M. Azizi, M. Mohamadian, and R. Beiranvand, "A new family of multi-input converters based on three switches leg," *IEEE Trans. Ind. Electron.*, vol. 63, no. 11, pp. 6812–6822, Nov. 2016.

[116] O. Ray and S. Mishra, "Boost-derived hybrid converter with simultaneous DC and AC outputs," *IEEE Trans. Ind. Appl.*, vol. 50, no. 2, pp. 1082–1093, Mar. 2014.

[117] B. Ge, "An energy-stored quasi-Z-source inverter for application to photovoltaic power system," *IEEE Trans. Ind. Electron.*, vol. 60, no. 10, pp. 4468–4481, Oct. 2013.

[118] M. Sarhangzadeh, S. H. Hosseini, M. B. B. Sharifian, and G. B. Gharehpetian, "Multiinput direct DC–AC converter with high-frequency link for clean power-generation systems," *IEEE Trans. Power Electron.*, vol. 26, no. 6, pp. 1777–1789, Jun. 2011.

[119] G. Teck Chiang and J.-I. Itoh, "A three-port interface converter by using an indirect matrix converter with the neutral point of the motor," in *Proc. IEEE Energy Convers. Congr. Expo.*, Sep. 2009, pp. 3282–3289.

[120] M. Rivera, S. Toledo, U. Nasir, A. Costabeber, and P. Wheeler, "New configurations of power converters for grid interconnection systems," in *Proc. IEEE Int. Conf. Automatica (ICA-ACCA)*, Oct. 2016, pp. 1–8.

[121] P. W. Wheeler, J. Rodriguez, J. C. Clare, L. Empringham, and A. Weinstein, "Matrix converters: A technology review," *IEEE Trans. Ind. Electron.*, vol. 49, no. 2, pp. 276–288, Apr. 2002.
[122] L. Empringham, J. W. Kolar, J. Rodriguez, P. W. Wheeler, and J. C. Clare, "Technological issues and industrial application of matrix converters: A review," *IEEE Trans. Ind. Electron.*, vol. 60, no. 10, pp. 4260–4271, Oct. 2013.
[123] J. Monteiro, J. F. Silva, S. F. Pinto, and J. Palma, "Linear and sliding-mode control design for matrix converter-based unified power flow controllers," *IEEE Trans. Power Electron.*, vol. 29, no. 7, pp. 3357–3367, Jul. 2014.
[124] F. Zare, H. Soltani, D. Kumar, P. Davari, H. A. M. Delpino, and F. Blaabjerg, "Harmonic emissions of three-phase diode rectifiers in distribution networks," *IEEE Access*, vol. 5, pp. 2819–2833, 2017.
[125] Y. Shi, L. Liu, H. Li, and Y. Xue, "A single-phase grid-connected PV converter with minimal DC-link capacitor and low-frequency ripple-free maximum power point tracking," in *Proc. IEEE Energy Convers. Congr. Expo.*, Sep. 2013, pp. 2385–2390.
[126] H. Zhu, D. Zhang, Q. Liu, and Z. Zhou, "Three-port DC/DC converter with all ports current ripple cancellation using integrated magnetic technique," *IEEE Trans. Power Electron.*, vol. 31, no. 3, pp. 2174–2186, Mar. 2016.
[127] Z. Chen, Q. Wu, M. Li, Y. Xu, and Q. Wang, "A three-port DC-DC converter with low frequency current ripple reduction technique," in *Proc. IEEE Appl. Power Electron. Conf. Expo. (APEC)*, Mar. 2015, pp. 2069–2074.
[128] H. Hu, X. Fang, F. Chen, Z. J. Shen, and I. Batarseh, "A modified high-efficiency LLC converter with two transformers for wide input-voltage range applications," *IEEE Trans. Power Electron.*, vol. 28, no. 4, pp. 1946–1960, Apr. 2013.
[129] J. Deng, S. Li, S. Hu, C. C. Mi, and R. Ma, "Design methodology of LLC resonant converters for electric vehicle battery chargers," *IEEE Trans. Veh. Technol.*, vol. 63, no. 4, pp. 1581–1592, May 2014.
[130] N. Hou and Y. W. Li, "Overview and comparison of modulation and control strategies for a nonresonant single-phase dual-active-bridge DC–DC converter," *IEEE Trans. Power Electron.*, vol. 35, no. 3, pp. 3148–3172, Mar. 2020.

MD. MEJBAUL HAQUE (Senior Member, IEEE) received the B.Sc. degree in electrical and electronic engineering (EEE) from the Rajshahi University of Engineering & Technology (RUET), in 2010, the M.Sc. degree in electrical and electronic engineering (EEE) from the Khulna University of Engineering & Technology (KUET), Bangladesh, in 2013, and the Ph.D. and M.Eng. degrees in electrical engineering from CQUniversity, Australia, in 2016 and 2020, respectively. He is currently a Research Fellow/a Lecturer with the School of Information Technology and Electrical Engineering (ITEE), The University of Queensland (UQ), Brisbane, Australia. Prior to joining UQ, he was a Research Fellow with the School of Engineering, Australian National University (ANU). He led the technical research of Realizing Electric Vehicle-to-Grid Services (REVS) Project with a total budget of $6.59m at ANU which was funded by Australian Renewable Energy Agency (ARENA) and ACT Government. He has been with CQUniversity as an Adjunct Research Fellow, since 2021. He started his professional career as a Lecturer with the EEE Department, KUET, in June 2010, and was promoted to an Assistant Professor, in September 2013. He has authored or coauthored more than 40 technical papers, including book chapters, journals, conference papers, and industry reports in electrical engineering. His research interests include power quality, power electronics, renewable energy technologies, and smart grid.

He served in the Organizing Committee of past IEEE SPEC 2020, IEEE i-COSTE 2020, and IEEE i-COSTE 2021 as the Student Activities Chair and Industry and the Local Arrangement Co-Chair. He was a recipient of the Best Paper Award in IEEE R10 HTC 2017 and received travel grants in IEEE R10 HTC 2017, IEEE IAS 2019, and IEEE PESGRE 2020 conferences. He is a member of Engineers Australia and a Registered Professional Engineer in the State of Queensland. He is an Associate Editor of IEEE Access journal.

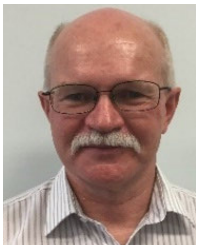

PETER J. WOLFS (Senior Member, IEEE) is currently with the School of Engineering and Technology, Central Queensland University. His research interests include power electronics applications for solar energy, smart grid technology especially distributed renewable resources and energy storage impacts on system capacity, and power quality. He is a fellow of Engineers Australia and a Registered Professional Engineer in the State of Queensland.

SANATH ALAHAKOON (Member, IEEE) received the B.Sc. (Eng.) degree (Hons.) in electrical and electronics engineering from the University of Peradeniya, Sri Lanka, in 1994, and the Ph.D. degree in digital motion control from the Electrical Machines and Power Electronic Group, The Royal Institute of Technology (KTH), Sweden, in 2000. Currently, he is a Senior Lecturer in electrical engineering with the School of Engineering and Technology, CQUniversity, Australia. His research interests include machines and drives, digital control, estimation and identification, non-linear control, instrumentation, automation, renewable energy, micro grids, and hybrid electric systems.

MD. ARIFUL ISLAM received the B.Sc. degree in electrical and electronic engineering (EEE) from the Ahsanullah University of Science and Technology (AUST), Dhaka, Bangladesh, in 2013, and the M.Eng. degree in electric power system management (EPSM) from the Asian Institute of Technology (AIT), Thailand, in 2019. Since 2019, he has been an Assistant Professor with the Electrical and Electronic Engineering (EEE) Department, AUST. Prior to that, he also worked as an Assessor in electrical and fire safety in Sumerra, Bangladesh, which was an American Project under Alliance. His research interests include renewable energy technology and applications, power management, and load profile analysis on the distribution side. He was a recipient of the Asian Development Bank-Japanese Scholarship Program (ADB-JSP) Scholarship to pursue his M.Eng. degree at AIT.

MITHULAN NADARAJAH (Senior Member, IEEE) received the Ph.D. degree in electrical and computer engineering from the University of Waterloo, Canada, in 2002. He worked as an Electrical Engineer with the Generation Planning Branch of Ceylon Electricity Board, Sri Lanka, and the Research Leader of Chulalongkorn University, Bangkok, Thailand. He is currently an Associate Professor with The University of Queensland (UQ). He is also the Director of Research Training and the Postgraduate Coordinator with the School of Information Technology and Electrical Engineering, UQ. He also worked as the Coordinator of Energy Field of Study and the Director for the Regional Energy Resource Information Center (RERIC), Asian Institute of Technology, Bangkok. His research interests include grid integration of renewable energy and energy storage systems.

FIRUZ ZARE (Fellow, IEEE) received the Ph.D. degree in power electronics from the Queensland University of Technology, Australia, in 2002. He is currently a Power Electronics Professor and the Head of the School of Electrical Engineering and Robotics, Queensland University of Technology. He has over 20 years of experience in academia, industry, and international standardization committees, including eight years in two large research and development centres working on power electronics and power quality projects.

He has received several awards, such as an Australian Future Fellowship, John Madsen Medal, Symposium Fellowship, and Early Career Excellence Research Award. He has published four books, over 280 journals and conference papers, five patents, and over 40 technical reports. He is also the Task Force Leader (the International Project Manager) of Active Infeed Converters to Develop the First International Standard IEC 61000-3-16 within the IEC Standardization SC77A. He is a Senior Editor of IEEE ACCESS journal, a Guest Editor and an Associate Editor of the IEEE JOURNAL OF EMERGING AND SELECTED TOPICS IN POWER ELECTRONICS, an associate editor of IET journal, and an editorial board member of several international journals. His research interests include power electronics topology, control and applications, power quality and regulations, and pulsed power applications.

OMAR FARROK (Member, IEEE) received the B.Sc., M.Sc., and Ph.D. degrees from the Rajshahi University of Engineering & Technology, Rajshahi, Bangladesh, in 2006, 2009, and 2016, respectively, all in electrical and electronic engineering (EEE). He was promoted to a Full Professor with the Department of EEE, Ahsanullah University of Science and Technology, Dhaka, Bangladesh, in 2020. He has authored or coauthored more than 80 technical papers in the international journals and conference proceedings, including 12 IEEE TRANSACTIONS/journal articles. His research interests include permanent magnet machines, linear electrical generator, magnetic material, renewable energy systems, oceanic wave energy converter, electrical machine and drive, electromagnetics, and power electronics. He is also a Life Fellow of the Institution of Engineers, Bangladesh. He was a recipient of six best paper awards from the IEEE international conferences. He is elected as the Chair, the Co-Chair, and nominated as a member of several technical committees formed by the Bangladesh Government under the Ministry of Industries and others. He was a Professional Engineer with the Board of Bangladesh Professional Engineers Registration Board, in 2017.